# A Novel, Autonomous, Module-Based Surgical Lighting System

ANDRE MÜHLENBROCK, University of Bremen, Germany
HENDRIK HUSCHER, KIZMO GmbH, Germany
VERENA NICOLE USLAR and TIMUR CETIN, Carl von Ossietzky University of Oldenburg, Germany
RENE WELLER, University of Bremen, Germany
DIRK WEYHE, Carl von Ossietzky University of Oldenburg, Germany
GABRIEL ZACHMANN, University of Bremen, Germany

Optimal illumination of the surgical site is crucial for successful surgeries. Current lighting systems, however, suffer from significant drawbacks, particularly shadows cast by surgeons and operating room personnel. We introduce an innovative, module-based lighting system that actively prevents shadows using an array of swiveling, ceiling-mounted light modules. The intensity and orientation of these modules are autonomously controlled by novel algorithms utilizing multiple depth sensors mounted above the operating table. This paper presents our complete system, detailing the algorithms for autonomous control and the initial optimization of the light module setup. Unlike prior work that was largely conceptual and based on simulations, this study introduces a real prototype featuring 56 light modules and three depth sensors. We evaluate this prototype through measurements, semi-structured interviews (n=4), and an extensive quantitative user study (n=11). The evaluation focuses on illumination quality, shadow elimination, and suitability for open surgeries compared to conventional OR lights. Our results demonstrate that the novel lighting system and optimization algorithms outperform conventional OR lights for abdominal surgeries, according to both objective measures and subjective ratings by surgeons.

CCS Concepts: • **Applied computing** → **Health informatics**; • **Hardware** → *Sensor applications and deployments*; • **Computing methodologies** → *Reconstruction*; • **Mathematics of computing** → *Evolutionary algorithms.*

Additional Key Words and Phrases: surgical lighting, depth sensor, point cloud, optimization

**ACM Reference Format:**
Andre Mühlenbrock, Hendrik Huscher, Verena Nicole Uslar, Timur Cetin, Rene Weller, Dirk Weyhe, and Gabriel Zachmann. 2024. A Novel, Autonomous, Module-Based Surgical Lighting System. *ACM Trans. Comput. Healthcare* 1, 1 (October 2024), 30 pages. https://doi.org/10.1145/3696670

## 1 Introduction

Good illumination of the surgical site – i.e. the wound – is crucial for the success of surgical interventions. Only with a well-illuminated surgical site are surgeons able to detect fine vessels easily, identify the cause of internal bleeding, and distinguish healthy tissue from malignant tumors. This leads to high demands on surgical lights in terms of illuminance and spectral properties, which are specified in standards (e.g. EN IEC 60601-2-41 [12]).

Authors' Contact Information: Andre Mühlenbrock, muehlenb@uni-bremen.de, University of Bremen, Bremen, Germany; Hendrik Huscher, KIZMO GmbH, Oldenburg, Germany; Verena Nicole Uslar; Timur Cetin, Carl von Ossietzky University of Oldenburg, Oldenburg, Germany; Rene Weller, University of Bremen, Bremen, Germany; Dirk Weyhe, Carl von Ossietzky University of Oldenburg, Oldenburg, Germany; Gabriel Zachmann, zach@cs.uni-bremen.de, University of Bremen, Bremen, Germany.


ACM 2637-8051/2024/10-ART
https://doi.org/10.1145/3696670

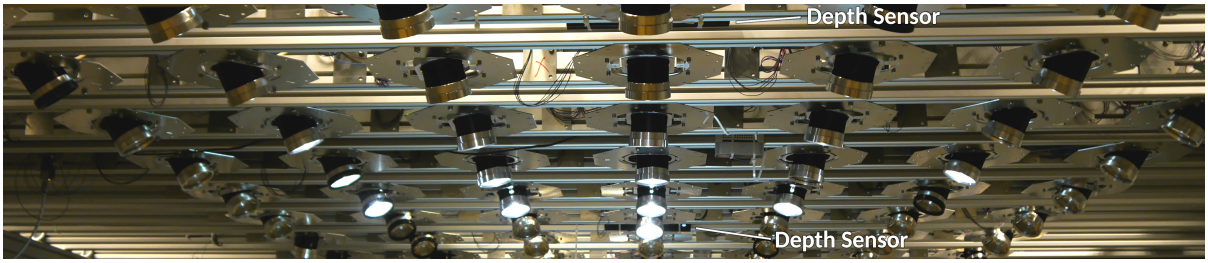


Fig. 1. Prototypical implementation of our novel, autonomous module-based lighting system for open surgery at the Pius Hospital Oldenburg, Germany.

One of the most commonly used lighting systems in open surgery is conventional overhead OR lights, which consist of two or three large lighting units suspended from the ceiling using a system of movable arms. Each individual lighting unit has a large surface area and is equipped with many small LEDs to generate shadows as soft as possible. In addition, the latest generation of lamps features shadow management that automatically dims some areas of the lighting units when they are partly occluded and increases the brightness of the remaining LEDs to keep the brightness on the site stable. Nevertheless, shadowing is still considered as one of the main problems using conventional OR lights, making it difficult to illuminate wounds and requiring frequent readjustment of the lighting units [23]. While alternative illumination methods such as headlights and lighted retractors (which are directly placed into the surgical site), largely solve the problem of shadowing, they come with other issues that affect ergonomics (carrying weight and inflexible posture of the surgeons) and patient safety (sterility and dangers of burns) [8].

In this paper, we present and evaluate a novel autonomous module-based lighting concept, implemented as a real-world prototype (see Figure 1), that effectively solves the problems of shadowing on the surgical site and the need for manual adjustments, and overcomes the limitations of existing illumination methods. Unlike conventional large lighting units, this system comprises numerous small swiveling light modules mounted on the ceiling. These modules automatically rotate and adjust their intensity, controlled by a central computer that receives real-time 3D information from multiple depth sensors around the OR table. Specifically, this paper addresses the following:

(1) The novel optimization algorithm that controls the individual light modules so that constant and shadow-free illumination of the surgical site is achieved.
(2) A novel method for determining optimal positions of the light modules; this method can be applied to both a specific operating room geometry, and to a set of surgery recordings so that the optimal illumination can be achieved in as many situations as possible.
(3) A comprehensive evaluation of our implementation of the lighting concept, including comparisons to a conventional surgical lighting system. Specifically, we investigate (a) the ability to *actively* prevent shadows cast by heads and bodies of OR staff using our algorithm, (b) the ability to *passively* reduce shadows cast by hands and medical instruments, and (c) the suitability of the new lighting concept for open surgery, using both open-ended expert interviews (n=4 experts) and a quantitative laboratory comparative study (n=11 experts).

While we have previously investigated the autonomous control algorithm [30] and the initial optimization of the light module positions [31] exclusively through simulations, this paper presents a real prototype for the first time. Using this prototype, we are now able to compare the performance of the novel lighting concept against conventional OR lights in terms of illumination quality, shadow elimination, and suitability through measurements and studies.

As far as we know, no similar illumination systems or algorithms have been presented in the scientific community with which we can directly compare our system. For this reason, we benchmark our illumination system against conventional OR lights. Our results demonstrate that this novel, autonomous, module-based lighting concept, combined with our novel algorithms, is more suitable for open surgery than conventional surgical lights in terms of illuminating a surgical field.

## 2 Related Work

In this section, we give an overview of the current state of lighting in open surgery (Section 2.1), ideas from research to improve conventional OR lights (Section 2.2), research on new module-based illumination approaches (Section 2.3), optimization problems in general (Section 2.4), and implemented optimizations for better and more efficient illumination of surfaces in various contexts (Section 2.5).

### 2.1 Current State of Surgical Lighting

In today's operating rooms, conventional OR lights are commonly used for traditional open surgery. At the same time, good illumination of the surgical wound is one of the major issues described by surgeons during surgery in order to perform their work accurately, productively, and safely [33]. According to Knulst et al. [23], conventional OR lights are readjusted every 7.5 minutes on average to provide appropriate illumination for the surgical site causing a significant distraction and accumulation of interruptions in the surgical procedure. In addition, surgeons and other OR personnel often saw a need for improvement in lighting intensity, shadowing, illumination of deep wounds, and the handling of such lights. Matern and Koneczny [27] highlight similar drawbacks of conventional OR lights, whereby the risk of inadequate illumination in the event of unexpected bleeding, as well as collisions between the surgeons and the light leading to blackouts, concussions, or lacerations was examined. Curlin and Herman [8] elaborate on the advantages and disadvantages of common surgical lighting methods, which in addition to conventional OR lights include headlights, illuminated retractors, and surgical microscopes, none of which meet all lighting requirements. In particular, it is described that headlights are often not used by surgeons due to their non-optimal illumination as well as the strain on the head and neck; likewise, the cables are often perceived as limiting, as with lighted retractors. Similar to laparoscopic fiber optic cables, the fiber optic cables connected to lighted retractors and headlights pose a safety risk to the patient in the form of burns and fires [3][16][15].

While good illumination and the absence of shadows are often seen as the main objective when illuminating a surgical site (e.g. [1][23][8]), the experiments in [24] are indicating that the selective use of shadows might improve the surgeon's depth perception in particular for objects very close to the surgical site, albeit the clinical relevance has not been investigated. Our prototype takes this into account since shadows from nearby objects like hands are not actively and thus never completely removed, as visible in Figure 13e.

Recently, the impact of the necessity of manual operation of a surgical light on performance and mental load during an attention test was examined in [5], indicating an advantage of autonomous lights in terms of reducing mental load.

### 2.2 Approaches for Improving Conventional OR Lights

To solve the disadvantages of handling and shadows with conventional OR lights, some approaches have been presented in the past decades: Choi et al. [6] proposed to use an illumination robot to automatically position and align the light source to avoid shadows cast by the surgeon's head. For this purpose, the position and rotation of the surgeon's head were detected with the help of ultrasonic sensors attached to the head. As an approach to improve the handling of conventional OR lights, Dietz et al. [9] suggest using a gesture control for brightness and color temperature instead of using a control panel, which is usually located high up on the conventional OR light.

Joseph and Divya [18] use a glove to recognize gestures that also allow positioning of the light in the operating room. In [37], the idea of fully autonomous positioning and rotation of multiple OR lights simultaneously was continued: A time-of-flight depth sensor was used to detect the OR personnel, thus avoiding the need for the personnel to wear sensors on the body. Moreover, the used optimization procedure was further improved in [38], which weighs the optimization objectives of "as optimal light as possible" versus "as little movement of the OR lights as possible". In [4], an autonomous surgical light is presented that integrates wound field detection using thermal cameras. However, this wound field detection is limited to the location of the wound and does not account for its depth or orientation, which is crucial for ensuring proper depth illumination. We considered developing a similar motor-driven approach, but decided against pursuing this approach further due to several drawbacks, including expected noise, space requirements, and the danger of collisions with OR personnel as stated in [27]. Additionally, there is a risk that surgeons and medical staff may not notice the automatic repositioning of such motor-driven OR lights and could inadvertently bump into them. We concluded that autonomous motor-driven surgical lights are not suitable for real operating rooms.

In addition, to improve the handling and shadow-free illumination of surgical lights, there are other aspects that have been addressed in the research regarding OR lights: Shen et al. [35] and Wang et al. [40] sought to optimize the spectral properties of the light source so that the textures of the tissue were more visible to the surgeons, and Knulst et al. [22] adapt the shape of the illuminated area to the shape of the real surgical site using bendable LEDs inside a surgical light.

## 2.3 Module-based Lighting Systems

In novel lighting concepts for operating rooms (e.g. the concepts mentioned in the introduction or those covered by a patent [10]), a variety of small lighting modules are proposed that are placed on the ceiling and control themselves to automatically generate optimal illumination at the site and avoid shadowing by using depth sensors. There has recently been a system on the market from Optimus Ise called Celestial™ Surgical Lighting System that comes close, but there doesn't seem to be any active compensation for shadows there.

Recently, we presented an optimization procedure in [31] to position only-slewable but non-moveable light modules of such lighting systems on the ceiling in such a way that the most satisfactory illumination is theoretically reachable during various surgeries. Finally, in [30], we presented a runtime optimization of the intensity of such a module-based lighting system for active shadow avoidance. There, we demonstrated through simulations that the module-based lighting concept with active autonomous intensity control performs better in large, shallow surgical wounds and significantly better in small, deep wounds compared to uniformly controlling all light modules to achieve the desired target brightness. However, as far as we know, a comparable autonomous lighting concept has not yet been compared to currently used OR lights, either through simulations or with a real prototype.

## 2.4 Optimization Problems

To find a solution for optimization problems for which no performant optimal algorithm is known, countless methods have been presented in the literature, especially metaheuristics, which can be applied to a wide range of problems. Examples are *Genetic Algorithms* [17], *Simulated Annealing* [21], *Particle Swarm Optimization* [20], *Artificial Bee Colony* [19], the *Grey Wolf Optimizer* [28] and many more, for which many variants exist (e.g. [36], [11], [34] etc.) and which continues to be an active field of research. Since metaheuristics can be very slow, greedy algorithms are frequently used, which can provide optimal or at least very good results in a short time for many problems [7]. According to the No Free Lunch Theorem (NFL), there is no single algorithm that is equally suitable, optimal, and fast for every class of optimization problem [44] – the choice of algorithm is, therefore, decisive and may not be trivial for solving a specific optimization problem.

An essential aspect of optimization is the consideration of constraints – the limitation of the range of values of parameters, possibly also interdependent. When using algorithms that do not natively account for constraints, such as genetic algorithms, penalties in various forms are often added to the function being optimized if a constraint is violated which are discussed for example in [45].

### 2.5 Optimizing the Illumination of a Surface

In the context of open surgery, [37] and [38] describe a concept for automatically optimizing the position of three motor-driven light units of conventional OR lights during surgery – however, this idea was only tested virtually and would have some disadvantages in reality, such as the risk of collisions with OR personnel and the expected noise level. In scenarios other than medical surgeries, optimization of illumination of surfaces is also performed: For example, Pachamanov and Pachamanova [32] pose a linear optimization problem to optimize the light distribution in tunnels and public roads by multiple luminaires. Another example is the reduction of energy consumption by selectively optimizing the brightnesses of multiple light modules in office spaces while maintaining user satisfaction, as done in [41] and [43].

## 3 The Lighting Concept

### 3.1 General Concept

Our new module-based lighting concept uses an array of many small light modules mounted on the ceiling, which are automatically controlled in intensity and rotation, while their positions are fixed (see Figure 2). In this system, surgeons can specify their preferred intensity, the point of interest to which all light modules are automatically aligned, and the desired angle of incidence of the light. This can be done, for example, sterilely via voice and gesture control as examined in [46], or non-sterilely using a tracked pen with infrared markers or via a graphical user interface. However, user control is not a focus of our paper and is addressed by Zargham et al. [46].

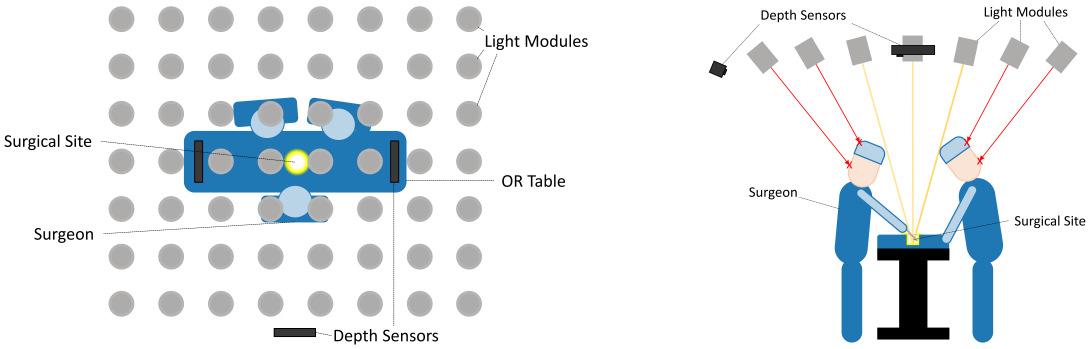


Fig. 2. Schematic illustration of our proposed module-based lighting concept for OR rooms. Left: top-down view, right: side view.

The system also consists of several depth sensors (e.g. , Microsoft Kinect) that can detect the OR personnel and objects in the area of the OR table. The geometric data recorded in this way is used to automatically determine which light modules can illuminate the site and the light modules from which the light is blocked. Light modules whose light is blocked can be switched off, and the remaining light modules can compensate for the lost intensity. In this way, the lighting system actively and automatically prevents shadows from being cast by the heads and bodies of the OR personnel.

However, to avoid too fast light changes, which could disturb the surgical procedure, the light only reacts to objects outside a certain radius $r$ (in our case $r = 0.3$ m) around the surgical site and thus not to hand movements close to the site. Nevertheless, hand shadows and shadows by medical instruments can be significantly reduced, too, compared to conventional OR lights due to the large number of simultaneously illuminated light modules distributed over a large area on the ceiling, as pointed out in Section 6.

### 3.2 Prototypical Implementation

We have implemented an actual prototype of the lighting concept at the Pius Hospital Oldenburg, Germany (see Figure 1). The prototype consists of 7 x 8 light modules placed in a grid-like pattern on the ceiling at a distance of 0.36 m x 0.35 m (as shown in Figure 2). Each light module is dimmable, rotatable by two motors, and able to produce an illuminance of about 45 klx at a distance of 2 m in the center of the illuminated area. We use three Microsoft Kinect v2 as depth sensors, two of which we mounted between the light module array and another one laterally behind the surgeon (see Figure 2), which were connected to a single computer that processes our algorithm presented in Section 5 in real-time. Moreover, the computer is connected to control boards that eventually control the motors and the power feed to the LEDs.

### 3.3 ToF Camera Accuracy and Interference

While depth cameras exhibit very high accuracy along their x and y axes (image plane) with proper intrinsic calibration, higher variations typically occur along the z-axis when projecting pixels into 3D space. [42] compares the accuracy of these depth cameras, showing that the standard deviation for the Microsoft Kinect v2 we used is within a few millimeters. The largely constant offset described there is indirectly corrected in our system through registration with [29]. By focusing the registration in the area above the operating table, we ensure that the accuracy is maximized in this critical region.

Although previous studies, such as [25] and [26], indicate potential interference issues with multiple Time-of-Flight cameras like the Microsoft Kinect v2 under certain circumstances, we did not identify any significant interference in our setup that exceeded the usual noise levels of such sensors, nor did it impact our algorithms. To counteract noise and potential interference in general, we incorporated a 1D Kalman filter in our algorithms for the occlusion testing of each light module (see Section 5.1). Additionally, the depth cameras are positioned on the ceiling and oriented towards the surgical site, similar to the light modules, to further reduce the impact of noise and potential interference that occurs along depth direction of the camera.

## 4 Optimal Positioning of Light Modules

When planning and installing such a module-based surgical lighting system, it is essential to determine the number and positioning of the lighting modules, as their positions remain static in our concept. Possible arrangements are grid-like or hexagonal placements in which the modules are all equally spaced. The spacing is selected so that at least the desired illuminance is always achieved in all desired positions and orientations where the surgical site might be during surgery – this is what we did in the actual prototype, see Section 3.2.

Nevertheless, it may be helpful to further optimize the positions to the peculiarities of an operating room as well as to the characteristics of different types of surgery: In [31], we have presented a method where the positions of the light modules are optimized on actually performed surgeries, which are recorded beforehand using depth sensors. The optimization method is described in Section 4.1, a study using recordings of nine real open abdominal surgery recordings are presented in 4.2, the results are shown in Section 4.3 and are discussed in Section 4.4.

## 4.1 Optimization

The goal of this section is to investigate the impact of different arrangements of light modules on the achievable lighting quality before the installation and construction of the prototype, and to optimize these arrangements accordingly, ensuring the best possible lighting for a variety of surgeries. We use recordings of a set of actual surgeries as input for our optimization. These recordings consist of depth images of one or multiple depth sensors. To perform the optimization efficiently, the depth recordings from multiple sensors are pre-processed. Depth images from multiple sensors with the same timestamp are projected onto a common heightmap in precisely the same way as described in detail in the optimization pipeline for *runtime optimization* in Section 5.1. This way, we obtain a heightmap, each for a specific point in time of the surgery.

During optimization, these pre-processed heightmaps are used to check whether individual rays between the light modules and individual points on the surface of the surgical site are blocked by objects or OR personnel. Using this occlusion information, we can approximate how brightly the surgical site is illuminated in the center – we then use this brightness in our score function. Since we want to optimize not only *a single point of time for one specific surgery* but on *all* situations of a set of surgeries, we consider not only one heightmap $h_i$ but the brightness on all heightmaps $h_i \in H$ for an *arrangement of light modules* $L$. Furthermore, we want to obtain as bright light as possible in all situations, which is why we always optimize for the worst surgery situation using minimal brightness over all situations. Finally, the objective function which is to be maximized during optimization can be described as follows:

$$f_{\text{Min}}(L, H) = \min(\text{brightness}(L, h_0), ..., \text{brightness}(L, h_n))$$

Note that the use of the minimum brightness over all situations also has the advantage that an over-representation or under-representation of individual situations in the available surgery recordings has much less influence, as would be the case, for example, with the average brightness over all situations ($f_{\text{Avg}}$). After all, in each iteration step, only the worst performing situation is optimized while other possibly overrepresented situations have no influence on the objective function, as would be the case with $f_{\text{Avg}}$.

Due to different requirements that may be imposed on such a system, we distinguish between two optimization problems:

(1) *Fixed-Layout Problem*: Possible positions for the light modules on the ceiling are often predefined both by the operating room and by design (e.g. , by the suspension or sockets for modules). In this case, the best $n$ positions for the light modules must be selected from a limited set of $m$ positions. The *Fixed-Layout Problem* describes the selection of the $n$ best positions from these $m$ possible positions.
(2) *Free-Layout Problem*: We also consider the case that the OR room can be planned and built around the lighting system, i.e. the modules can be placed arbitrarily. This *Free-Layout Problem* allows the free placement of $n$ light modules with the only constraint that a minimum distance $c$ (we used $c = 0.32\,\text{m}$) between all light modules is maintained.

## 4.2 Study

We performed recordings with three depth sensors (Microsoft Kinect v2) of nine actual open abdominal surgeries together with the Pius Hospital Oldenburg, Germany (see Figure 3). To reduce the computational time we reduced the sample rate of depth images to one depth image per 2 minutes, resulting in 519 considered heightmaps of 17.3 hours of active surgery. These nine surgeries included gastrectomy, bowl surgeries (including preparation of ileostomy/colostomy) and hepatic tumor removal. The situations in which light is less demanding were not included (i.e. , surgical preparations such as draping with drapes or final procedures such as suturing the surgical wound). During these surgeries, conventional OR lights with two moving light units were used, which were partially visible in the depth recordings but were cropped out using a height threshold of 1.95 m – since no

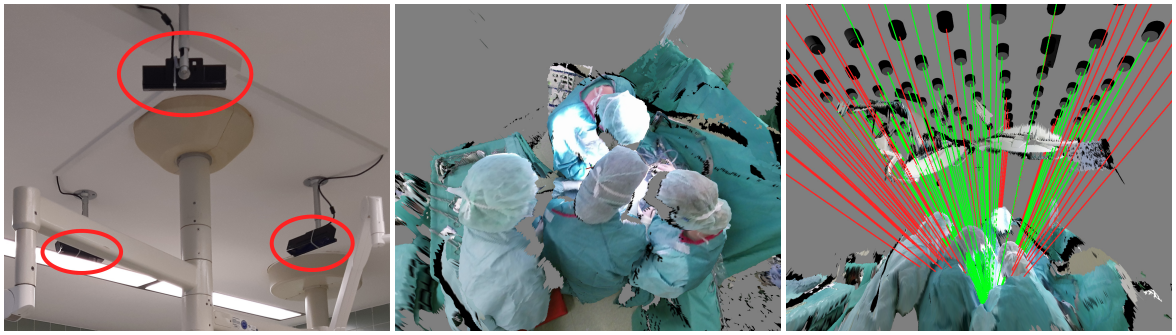

Fig. 3. Creating depth recordings of nine real open abdominal surgeries and using them for ray tests in our optimization procedure. Left: Installation of depth sensors in the surgery room; middle: combined 3D point cloud recorded by these depth sensors; Right: Performing ray tests from light modules at the ceiling to the surgical site against the point cloud, while the conventional OR lights, which is partly visible in the point cloud, was omitted during optimization by using a height threshold of 1.95 m. The occlusion test is internally performed against a height map while the original three overlapping registered point clouds are displayed here. First published in [31], © SPIE.

surgeon exceeded this height, this was not a problem. The surgical sites, which were at slightly different positions in all nine surgeries, were determined manually, and all light modules were assumed to shine exactly onto the midpoint of the surgical site during optimization.

For both optimization problems, we designed realistic scenarios and utilized appropriate optimization algorithms:

(1) In the case of the *Fixed-Layout Problem*, we assumed a suspension that can hold (a) 100 light modules in a 10x10 grid-like arrangement and (b) 95 light modules in a hexagonal arrangement, each with a spacing of 0.32 m between light modules. In both cases, the 50 positions that lead to the best performance on the objective function should be determined. This results in $\binom{100}{50} \approx 10^{29}$ or $\binom{95}{50} \approx 2.8 \cdot 10^{27}$ possible combinations from which the one with the best results has to be chosen. Since this is not solvable in a reasonable amount of time and we assume a fairly well-structured optimization problem, we utilized a greedy algorithm that removed the light module that least reduces the result of the objective function in each iteration step. This way, we only had to evaluate the objective function on $\sum_{i=51}^{100} i = 3775$ configurations in the grid-like arrangement and on $\sum_{i=51}^{95} i = 3285$ configurations in the hexagonal arrangement, which is solvable within minutes on a recent computer.
(2) In the case of the *Free-Layout Problem*, we used the pagmo2 optimization library [2] and tested various heuristic optimization algorithms for a short time with a reduced number of heightmaps to get an indication of which algorithms might be particularly suited for this optimization problem – after all, according to the No Free Lunch Theorem [44], there is no best algorithm for every problem. We observed that (a) the Simple Genetic Algorithm (SGA), which is a custom implementation by pagmo2 of the genetic algorithm, and (b) the Self-adaptive Differential Evolution (SADE), an improved version of [36] that was inspired by Elsayed et al. [11], converged the fastest, which we limited to in the following for resource reasons. To integrate the distance constraint of c = 0.32 m between two light modules, we subtracted a penalty $p_{i,j}$ for each pair of light modules $i$ and $j$ that violated the constraint. The penalty was defined by $p_{i,j} = (c - d_{i,j}) \cdot a$, where $d_{i,j}$ is the distance between the light modules $i$ and $j$ and $a$ is a factor which we have chosen to be $a = 10000000$ after some experiments, so that a violation of 1 cm leads to a degradation of the objective function of 100 klx.

This way, both the amount of undercut distance and the number of pairs of light modules that undercut this distance were taken into account by the penalties applied.

To obtain a reliable measure of how effective the optimization is and, more importantly, how generalizable the optimized light module positions are, we performed a *leave-one-out cross-validation (LOOCV)*. For each recording $r_i$ of the nine surgeries, we performed an optimization exclusively using all the other surgery recordings as a training set while the recording $r_i$ was used as a test set. This allows us to test how well the optimized lamp positions perform with unknown surgical teams, surgeries, and surgical site positions. The cross-validation was performed on four optimization configurations shown in Table 1. Finally, we compared the LOOCV results with two lattice-like arrangements (G49 and G100) and two hexagonal arrangements (H46 and H95), respectively, which we also call *naive arrangements* hereafter and are visualized in Figure 5.

Table 1. List of optimization configurations on which the LOOCV was performed. Note that the number of light modules is iteratively reduced using the *Fixed-Layout Problem* while the number of light modules is unchanged when using the *Free-Layout Problem*. First published in [31], © SPIE.

| | | | Light Module Count | | |
|---|---|---|---|---|---|
| **Name** | **Algorithm** | **Type** | **Initial** | **Target** | **Initial Arrangement** |
| Greedy (Grid) | Greedy | Fixed-Layout Problem (a) | 100 | 50 | G100 (see Fig. 5) |
| Greedy (Hex) | Greedy | Fixed-Layout Problem (a) | 95 | 50 | H95 (see Fig. 5) |
| SGA | SGA | Free Layout Problem (b) | 50 | 50 | Random |
| SADE | SADE | Free Layout Problem (b) | 50 | 50 | Random |

## 4.3 Results

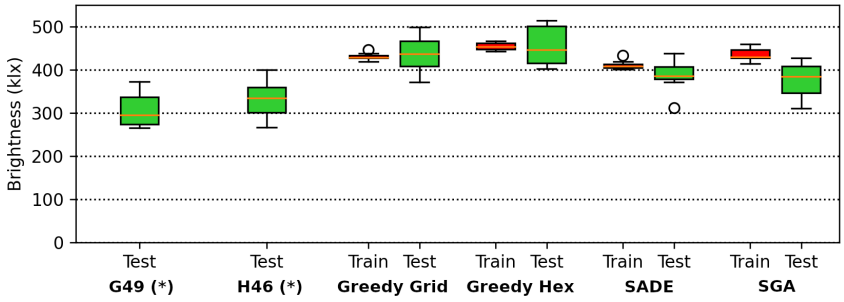


Fig. 4. Cross-validation results on training and test sets: Average of minimum brightness of all surgeries on the training set (red) and the test set (green). First published in [31], © SPIE.

The results of our *leave-one-out cross-validation* (LOOCV) are shown in detail in Table 2 and plotted in Figure 4. In both the *Fixed-Layout Problem* and the *Free-Layout Problem*, a significantly higher minimum brightness is archived over all frames compared to naive arrangements. Comparing the naive grid-like arrangement G49 with the optimized Greedy (Grid) arrangement, there is on average a 41 % increase from 307 klx to 433 klx in minimum brightness, normalized to the number of lights. The comparison between the H46 hexagonal arrangement

Table 2. Cross-validation results on test sets: Minimum brightness on test sets for different light module arrangements. To allow for a sensible comparison of the light module configuration despite different numbers of light modules, we calculated an efficiency value, defined as Efficiency = Mean ∗ (50/Num Lights). This value describes the approximate brightness of the illumination if the arrangement were sampled with 50 light modules. The "Rel. to G49 (*)" row indicates the efficiency increase compared to the arrangement G49. (All brightness values are given in kilo lux (klx)). First published in [31], © SPIE.

| | | **Naïve Arrangements** | | | | **Optimized Arrangements** | | | |
|---|---|---|---|---|---|---|---|---|---|
| **Test Set** | **Train Set** | **G49** | **G100** | **H46** | **H95** | **Greedy (Grid)** | **Greedy (Hex)** | **SADE** | **SGA** |
| Num Lights | - | 49 | 100 | 46 | 95 | 50 | 50 | 50 | 50 |
| Surgery 1 | 2-9 | 365 | 756 | 367 | 829 | 498 | 484 | 438 | 423 |
| Surgery 2 | 1, 3-9 | 289 | 608 | 307 | 649 | 467 | 501 | 372 | 427 |
| Surgery 3 | 1-2, 4-9 | 336 | 721 | 359 | 735 | 409 | 404 | 378 | 409 |
| Surgery 4 | 1-3, 5-9 | 330 | 649 | 330 | 668 | 453 | 515 | 419 | 392 |
| Surgery 5 | 1-4, 6-9 | 260 | 579 | 276 | 646 | 375 | 403 | 312 | 311 |
| Surgery 6 | 1-5, 7-9 | 285 | 631 | 293 | 648 | 371 | 415 | 394 | 347 |
| Surgery 7 | 1-6, 8-9 | 309 | 588 | 320 | 653 | 437 | 447 | 386 | 369 |
| Surgery 8 | 1-7, 9 | 267 | 551 | 245 | 543 | 412 | 422 | 379 | 345 |
| Surgery 9 | 1-8 | 268 | 628 | 262 | 643 | 471 | 509 | 407 | 385 |
| Mean | - | 301 | 634 | 306 | 668 | 443 | 456 | 387 | 379 |
| SD | - | 36 | 67 | 42 | 78 | 44 | 47 | 35 | 39 |
| **Efficiency** | - | **307** | **317** | **333** | **352** | **433** | **456** | **387** | **379** |
| Rel. to G49 (*) | - | **0 %** | 3 % | 8 % | 14 % | **41 %** | 48 % | 26 % | 23 % |

and greedy (Hex) results in a normalized 37 % increase in minimum brightness from 333 klx to 456 klx. These arrangements are the result of the *Fixed-Layout Problem*. While the results of the *Free-Layout Problem* also perform better than the naive arrangements with a minimum brightness of 387 klx and 379 klx, the increase in minimum brightness was on average much smaller than for the *Fixed-Layout Problem* optimizations.

These results suggest that there is much potential in optimizing the positions of the light modules in individual operating rooms as well as a selection of types of surgeries. In particular, the results indicate that the results are highly generalizable for surgeries of the same type, which take place in the same surgery room, and that the optimized lamp positions are also applicable to different surgical teams, surgeries, and positions of the surgical site. In a direct comparison between the naive G49 and H46 arrangements with the arrangements of the greedy optimization, we obtain significantly better normalized minimum brightness values not only on average but in almost every single surgery (see Table 2).

## 4.4 Discussion

*4.4.1 Limits of Optimization.* It may be surprising that the algorithms on the *Fixed-Layout Problem* perform better than the algorithms on the *Free-Layout Problem* since it is theoretically possible to obtain all possible arrangements with the *Free-Layout Problem* that can also be obtained with the *Fixed-Layout Problem*, while the

reverse is not the case. Looking not only at the results on the test set but also at the results on the training set (see Fig. 4), we find that SADE and SGA are inferior to the Greedy algorithm on the training set as well. This indicates that the *Free-Layout Problem* could not be solved optimally by the algorithms. The distance constraint might be one of the reasons for the worse performance. However, we must also consider that the search space in the *Free-Layout Problem* is much larger due to the infinite possibilities of positions for the light modules. This makes the *Free-Layout Problem* much harder to optimize in general compared to the *Fixed-Layout Problem*. From a practical perspective, the *Fixed-Layout Problem* might be even more relevant, as the possible positions for light modules are often limited - e.g. , by the scaffolding to which the light modules are attached or by ceiling-mounted sockets into which the light modules can be plugged.

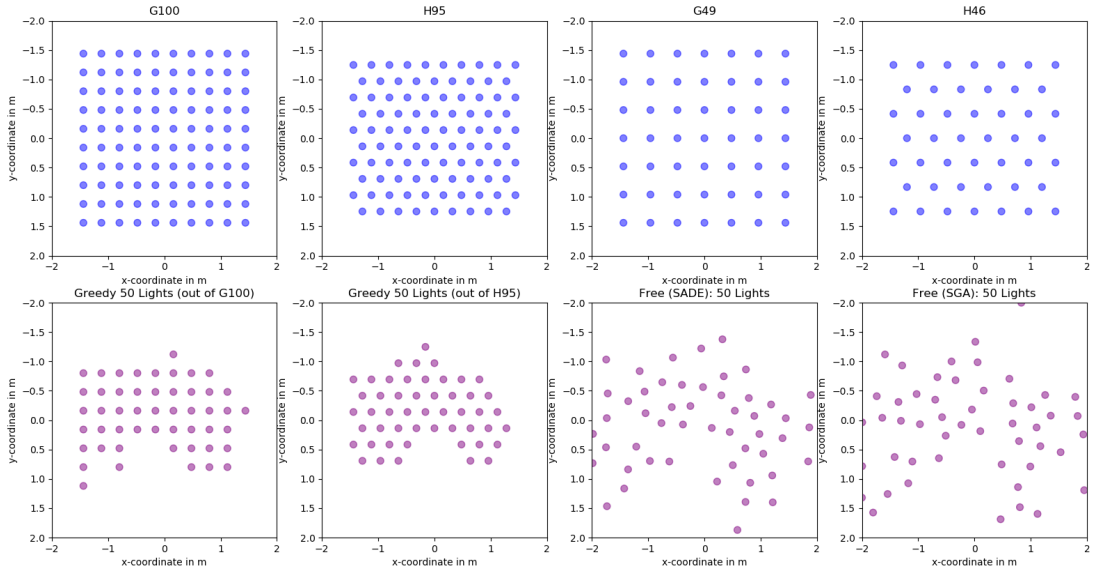


Fig. 5. Illustration of the arrangements used in the cross-validation for surgery 1. While the upper arrangements (blue) are the not-optimized naive arrangements which were identical for every surgery, the lower arrangements (purple) are the result of the optimization on surgery 2 – 9 (to test on surgery 1) and differ slightly for each surgery. First published in [31], © SPIE.

*4.4.2 Limitations.* It should be noted that the optimization results are still subject to some limitations, namely, on the one hand, that the surgeons used the conventional OR lights during the surgeries and also moved accordingly and likewise might have positioned themselves so that they did not block the light. Their moving pattern might differ from novel module-based lighting system approaches because surgeons no longer have to worry about casting shadows. On the other hand, the depth recordings used for the nine surgeries were not entirely complete in several frames due to occlusions from the conventional surgical lights – thanks to the use of the minimum function over all frames in the objective function, this might not create a general bias, but it could be that a few harder to illuminate situations were not fully considered due to incomplete depth images. Likewise, we did not consider a virtual site model because we had no reliable and detailed information about the depth and size of the surgical site in the surgery recordings (depth sensors are way not precise enough at that distance to the surgical site). Finally, we optimized exclusively on surgery recordings which were open abdominal surgeries, and they were all performed in a single OR room, so we do not know the extent to which the results are generalizable to other operating rooms and surgery types that are not open abdominal surgeries.

*4.4.3 Considerations.* We suggest that optimization be considered when planning a commercial module-based lighting system. In such a lighting system, sockets could be installed in the ceiling (e.g. , in the form of the G100 arrangement), into which only the desired number of light modules are inserted in the arrangement of the optimization result. This will allow easy repositioning of the light modules if the range of surgeries performed in the operating room changes significantly.

Installing depth sensors and making recordings to adapt the lighting system to the conditions of an operating room may sound like a lot of effort. However, such depth sensors are already integrated into such module-based surgical lighting systems, which could automatically record single frames during surgery, e.g. , record a depth image every minute (without color information and metadata to protect privacy) to perform both (a) general optimization across all operating rooms of a particular type to achieve an optimal initial setup during installation and (b) subsequent optimization for the respective operating rooms.

In the actual prototype, we decided against using an arrangement optimized on these surgery recordings, partly because of the just mentioned limitations, but also because of the following: (a) the optimized arrangements were trained in a different operating room and (b) quite different evaluations were to be performed (also by other research groups), where some of differed significantly in terms of the positioning of the persons present from the positions taken by the OR team in the surgery recordings, we could not say with certainty that an arrangement optimized on the nine surgery recordings would be more suitable than a uniform distribution of light modules in our use case. However, we were inspired by the results of these optimizations when arranging the light modules of the actual prototype: The optimization results show that the light modules tend to be located along the operating table (see Figure 5) – for this reason, we have opted for a 7 x 8 instead of a 7 x 7 arrangement. Nevertheless, even though we did not precisely adopt the optimized results in the prototype, our results clearly indicate that optimization of the light module positions might be advantageous for an actual commercial product.

## 5 Intensity Optimization during Surgery

In this chapter, we present our real-time intensity optimization of all light modules, which avoids shadows and illuminates the surgical site uniformly over time. This work was previously published in [30], where the intensity optimization was evaluated on simulated data only. In Section 5.1, the whole optimization pipeline is presented, and in Section 5.2, the actual optimization step of the optimization pipeline is described in detail.

### 5.1 Optimization Pipeline

Our pipeline (see Figure 6) receives the depth images from multiple depth cameras as input. These depth images are transformed into 3D point clouds using the camera's intrinsic and extrinsic parameters. Then we transform the 3D point clouds from camera space into world space (the OR room) by using a registration which we obtained by the lattice registration procedure presented in [29].

To adopt a more general approach, we do not explicitly recognize objects or people—in other words, we do not identify the surgeon, assistants, hands, heads, or similar entities. Instead, we directly use the detected geometry from the depth sensors for occlusion testing through intersection tests with the 3D point cloud data. Since collision checks between rays and 3D point clouds may be quite demanding, we first transform the separate 3D point clouds of multiple depth sensors into a common height map. This height map stores the height from the ground in the 2 m x 2 m area around the operating table. While we transform the point clouds onto the height map, we ignore all points of the point cloud within a fixed radius $r$ ($r = 30$ cm) around the surgical site so that the lighting system does not react to hands and medical instruments as described earlier.

To check whether a ray between a light module and the surgical site is blocked, we simply project the ray into the height map and iterate over the resulting line. This way, we can efficiently calculate for each light module whether there is any occluding object on the path that would lead to shadows at the site. To be able to also

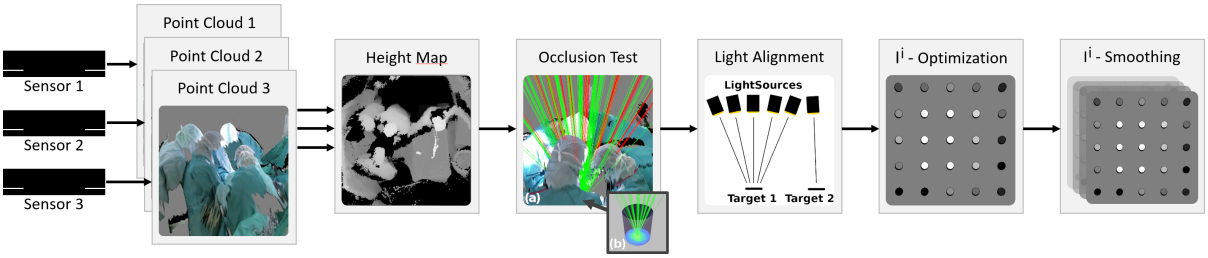


Fig. 6. Optimization pipeline: We first transform the depth images obtained from the depth sensors into three separate 3D point clouds and then map them onto a common height map. Occlusion tests are then performed for individual light modules against (a) the point cloud data (technically using the height map) and (b) a virtual cylindrical tube. The shading information is then used to adjust the alignment of the light modules, optimize the intensities, and smooth the intensities over time. Note that in this diagram, the point cloud is rendered with RGB values for illustrative purposes, although these are not used by the algorithm, which only uses 3D point data. First published in [30] by Springer Nature.

illuminate narrow, deep surgical sites well, we use a *virtual cylindrical tube* that is placed, rotated, and scaled to approximate the real surgical site. By performing ray tests not only against the point cloud but also against this virtual tube, we can ensure that only lights whose rays reach the bottom of the site are active. The ray-tube test is, in our case, very fast, since it can be reduced to a simple ray-disk intersection. By testing multiple rays per light module, which start at different positions on the luminous surface and end at different positions at the site, we moreover calculate a floating point value $vis^i$ that approximates how much light from a light module $i$ is blocked by the geometry. Moreover, we filter this value using a 1D Kalman filter to reduce sensor noise. In the next step, the light modules are assigned to a lighting target and rotated accordingly so that they shine onto the target. Finally, the intensities are optimized by using the floating point occlusion values $vis^i$ calculated for each light module $i$ – this is described in the following Section 5.2.

Note that as described before, the location, orientation, and size of the light target, which is enclosed by the geometry of the *virtual cylindrical tube*, is currently meant to be manually specified by the OR personnel via a GUI, a tracked pen or completely sterile via speech and gesture control as examined in [46].

## 5.2 Intensity Optimization Step

We designed a custom algorithm that calculates intensities for all light modules so that the light is kept as stable and constant as possible over time. We present the requirements of the algorithm in Section 5.2.1, the algorithm is explained in Section 5.2.2, a subsequent smoothing of the intensities is described in Section 5.2.3 and remarks are given in Section 5.2.4.

*5.2.1 Requirements.* To ensure that the illuminance $E_v$ at the surgical site remains as consistent as possible and close to the preferred value $E_{v_{\text{Pref}}}$, we must first calculate the illuminance $E_v^i$ produced by each individual light module $i$. This involves determining how different intensity levels $I^i$ of the light module affect the illuminance at the center of the site. Assuming the light falls perpendicularly and the distance $d_n$ is fixed, we use a mapping function $f$ that correlates the intensity $I^i$ of a light module with its illuminance $E_v^i$:

$$E^i_{v_{\text{Norm}}} = f(I^i) \tag{1}$$

This function $f$, based on measurements with a luxmeter at various power levels and fixed conditions, is assumed to be linear, indicating a uniform increase in intensity.

Further, to estimate the actual illuminance $E_v^i$ at the surgical site given the distance $d^i$ from light module $i$ to the center of the site, we consider the effects of distance and the angle of incidence. The normalized illuminance $E_{v_{\text{Norm}}}^i$ is adjusted for the quadratic decrease with distance and for the angle between the light vector $\vec{l}^i$ of the module and the virtual surface normal $\vec{n}$:

$$E_v^i = E_{v_{\text{Norm}}}^i \cdot \left(\frac{d_{\text{Norm}}}{d^i}\right)^2 \cdot (-\vec{l}^i \cdot \vec{n}) \tag{2}$$

Here, the factor $(-\vec{l}^i \cdot \vec{n})$ accounts for the decrease in illuminance due to any tilt in the surface, analogous to Lambert's cosine law, assuming that the amount of light remains constant over the surface area. This model allows us to fine-tune the intensity of each light module to achieve optimal illuminance across the surgical site.

*5.2.2 $I^i$-Optimization.* The algorithm is designed to optimize the distribution of light at a surgical site and consists of two primary steps. Initially, the light modules are ranked based on their effectiveness in illuminating the site, which is crucial for ensuring optimal lighting conditions. Following this, each non-occluded light module is incrementally assigned a specific amount of light until the desired brightness level is achieved, beginning with the most suitable module.

The ranking of light modules is determined through a scoring function that evaluates the perpendicularity between the inverse light vector $-\vec{l}$ and the site's surface normal $\vec{n}$. The assumption here is that the more perpendicular these vectors are, the more effectively the light can penetrate the surgical area, represented by the formula:

$$s_{Perpendicular}^i = (-\vec{l}_i \cdot \vec{n}) \tag{3}$$

An alternative scoring function was also considered in [30], which prioritized light modules based on their unobstructed view duration of the surgical site. However, this approach proved less effective for smaller sites and was subsequently abandoned.

Once the light modules are sorted by their suitability, the maximum possible illuminance $E_{v_{\text{MaxVis}}}$ at the site's center is calculated, factoring in any occlusions. This involves multiplying the maximum illuminance $E_{v_{\text{Max}}}^i$ each light module can provide by the proportion of unblocked light rays from that module to the site, and summing these values:

$$E_{v_{\text{MaxVis}}} = \sum^i E_{v_{\text{Max}}}^i \cdot vis^i \tag{4}$$

As described in the previous Section 5.1, $vis^i$ represents the fraction (in $[0, 1]$) of the light rays from light module $i$ that were able to reach the ground of the surgical wound during ray tracing, filtered by a 1D Kalman filter.

Prior to distributing light among the modules, a ratio $\omega$ is established to indicate the desired illuminance $E_{v_{\text{Pref}}}$ relative to the maximum illuminance achievable $E_{v_{\text{MaxVis}}}$:

$$\omega = \min(1, \frac{E_{v_{\text{Pref}}}}{E_{v_{\text{MaxVis}}}}) \tag{5}$$

A variable $E_{v_{\text{Rem}}}$, initialized with the preferred illuminance, represents the remaining required illuminance to achieve the target brightness:

$$E_{v_{\text{Rem}}} \leftarrow E_{v_{\text{Pref}}} \tag{6}$$

The system also incorporates a variable $\alpha$, which adjusts the distribution strategy from focusing on a few optimal, unblocked modules ($\alpha = 0.0$) to utilizing all available unblocked modules ($\alpha = 1.0$) to achieve the desired brightness.

During the iteration over sorted modules, the intensity $I^i$ for each module is calculated as follows:

$$I^i = I_{\text{Max}}^i(1 - \alpha) + I_{\text{Max}}^i \cdot \omega \cdot \alpha \tag{7}$$

The expected illuminance $E_v^i$ from each module is then computed using the given formulas and conditions:

$$E_v^{\mathrm{i}} = f(I^i) \cdot (\frac{d_{\mathrm{Norm}}}{d_i})^2 \cdot (-\vec{l_i} \cdot \vec{n}) \tag{8}$$

If the illuminance from a module is insufficient to meet the remaining requirement ($E_v^{\mathrm{i}} \leq E_{v_{\mathrm{Rem}}}$), it is subtracted from $E_{v_{\mathrm{Rem}}}$:

$$E_{v_{\mathrm{Rem}}} \leftarrow E_{v_{\mathrm{Rem}}} - E_v^{\mathrm{i}} \tag{9}$$

Conversely, if a module's output exceeds the remaining need ($E_v^{\mathrm{i}} > E_{v_{\mathrm{Rem}}}$), the intensity of that module is recalibrated, and the iteration stops after setting the remaining required illumination to zero:

$$I^i \leftarrow I^i \cdot \frac{E_{v_{\mathrm{Rem}}}}{E_v^{\mathrm{i}}} \tag{10}$$

*Note that our mapping function $f$ is linear. If $f$ were not linear, blending with $\alpha$ should not be based on the intensity $I^i_{Max}$ in (7). Instead, it should be done with the maximum expected illuminance $E^i_{v_{Max}}$, using an inverse function $f^{-1}$.*

**Algorithm 1** Light Optimization Step

```
sort(L)                                              ▷ Sort light modules by their suitability
E_vMaxVis ← Σ^i (E^i_vMax · unblockedRays(i))        ▷ Calculate the system's maximum possible illuminance
E_vRem ← E_vPref                                     ▷ Initialize remaining illuminance

ω ← min(1, E_vPref / E_vMaxVis)                      ▷ Calculate ratio (preferred illuminance: possible illuminance)

for every light module i do
    I^i ← I^i_Max(1 − α) + I^i_Max · ω · α           ▷ Set the initial luminous power for light i
    E^i_v ← f(I^i) · (d_Norm / d_i)^2 · (−l_i · n)   ▷ Calculate the expected illuminance by light i

    if E^i_v ≤ E_vRem then
        E_vRem ← E_vRem − E^i_v                      ▷ Subtract the luminance from the remaining luminance
    else                                             ▷ If the luminance is higher than the remaining luminance
        I^i ← I^i · E_vRem / E^i_v                   ▷ Scale it to fit the remaining luminance and break
        break
```

*5.2.3 $I^i$-Smoothing.* To avoid distracting surgeons by having the light react immediately to every movement around the site, we apply temporal smoothing to the intensity values $I^i$ for each light $i$. This is achieved by blending the previously smoothed intensities ${I_{\mathrm{Smoothed}}}^{i,t-1}$ from the previous frame $t-1$ with the optimal luminous power $I^{i,t}$ of the current frame $t$. The blending is controlled by a factor $\gamma \in (0, 1]$:

$${I_{\mathrm{Smoothed}}}^{i,t} = {I_{\mathrm{Smoothed}}}^{i,t-1} \cdot (1-\gamma) + I^{i,t} \cdot \gamma \tag{11}$$

*5.2.4 Remarks.* Currently, the optimization only considers the illumination at a single point, i.e. the center of the surgical site, although shadowing of multiple points is considered using the earlier described floating point value $vis^i$. However, it would also be possible to optimize the illumination for a whole surface area using multiple sample points: This is particularly useful if the emission characteristics of the light module are distributed unevenly over the surface (e.g. for cost reasons of the installed LED). Nevertheless, this optimization causes some problems: On the one hand, currently, our site model is only very coarse, mainly, because of the limited resolution and the fixed viewing angle of the depth sensors that cannot capture the complex geometry and details of real-world surgical sites. Moreover, the emission characteristics of the *actual physical light modules* – e.g. beam angle – cannot be changed. Consequently, the only way to compensate for uneven emission patterns remains the rotation of the light modules which would probably entail a constantly visible changing illumination. However, our optimization pipeline is already prepared to handle also such area-based optimizations as we are able to measure the illumination in multiple points at a site.

## 6 Investigating Shadowing

In this chapter, we present two experiments to compare the novel autonomous module-based lighting system to a conventional OR light (Dr. Mach LED 3) in terms of shadowing and shadow compensation. The first experiment examines the active compensation of *head* and *body* shadows by our intensity optimization (see Section 6.2), and the second experiment examines shadows by *hands* and *medical instruments* (see Section 6.3), which are meant to be passively reduced by using many light modules simultaneously over a large area on the ceiling. Both experiments were performed using the same measurement setup, presented in Section 6.1.

Note that in the following, the parameter $\alpha$ in the autonomous, module-based lighting system is the floating-point parameter discussed in Section 5.2.2. It controls the number of light modules used simultaneously, ranging from $\alpha = 0.0$, which corresponds to using as few light modules as possible, to $\alpha = 1.0$, which corresponds to using as many light modules as have an unobstructed view.

### 6.1 Measurement Setup

In both experiments, we used the same setup to measure brightness on an illuminated surface: We placed a camera in a constructed wooden box (see Figure 7). This box had a hole on the top, to which a white plastic plate was attached, through which light was almost exclusively transmitted diffusely. To minimize reflected light inside the box, the box was closed and painted dark from the inside. The system camera captured the light diffusing through the plastic plate at a resolution of 1280 x 720 pixels, operating at 50 fps, with both auto-exposure and auto-white balance features deactivated.

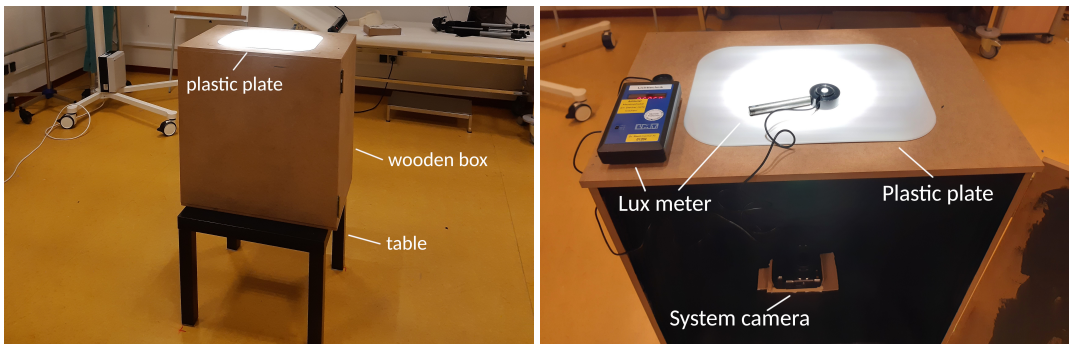


Fig. 7. Our setup to measure the illumination of different lighting conditions on a surface

To infer a brightness in lux (on top of the plastic plate) using the recorded RGB values from the camera placed below the plastic plate, we sampled random locations across the upper side of the plastic plate with a lux meter and fitted three polynomial functions that map the R, G, and B values to a lux value, respectively. To obtain a final lux value of a pixel, we used the weighted average of the results of the three separate functions. The average error of this resulting function was 3.6 % (SD: 3.4 %, Median: 2.4 %) using the 57 samples for calibration in a range of 2.5 klx to 64.8 klx (see Figure 8). Finally, we cropped the video to the area of interest of about 16 cm x 16 cm and downsampled it to a resolution of 24 x 24 pixels using the average of the surrounding pixels for data and noise reduction, giving us a total of 576 virtual lux sensors sampling at 50 Hz.

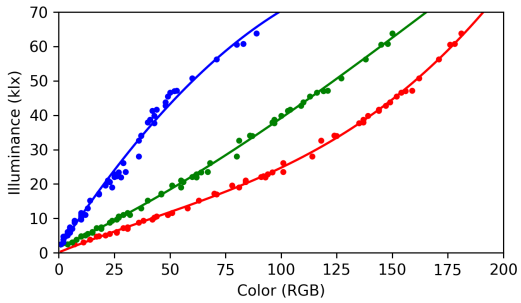


Fig. 8. Three color-to-illuminance mapping functions fitted into 57 samples measured with a luxmeter which are used to convert color values to illuminance. Since each function corresponds to a single color channel, we use the weighted average of all three functions to convert a pixel color into an illuminance value.

A surgical field may be illuminated with a maximum illuminance of up to 160 klx in order not to cause damage to the eyes [12]. Recommendations for the centrally illuminated area of the surgical site vary between 50 klx and 100 klx [14]. However, since no blood-red surgical site was illuminated in this both following experiments, but a purely bright plastic surface, we significantly reduced the brightness of the lighting systems to roughly 25 klx –35 klx in the center of the illuminated field in order not to cause glare to the test subjects.

## 6.2 Experiment 1: Active shadow avoidance

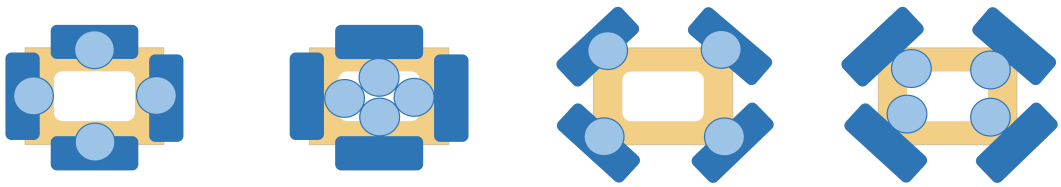


Fig. 9. Movement pattern with four people standing around the wooden box (top-down view). In each trial, people (a) stand in front of the sides of the box for 5 seconds, (b) bend forward for 5 seconds, (c) turn 45° and stand at the corners for 5 seconds, (d) bend forward again for 5 seconds, turn 45° again and so on. This is repeated until each person arrives at their original position, resulting in 32 movements at 5-second intervals per trial.

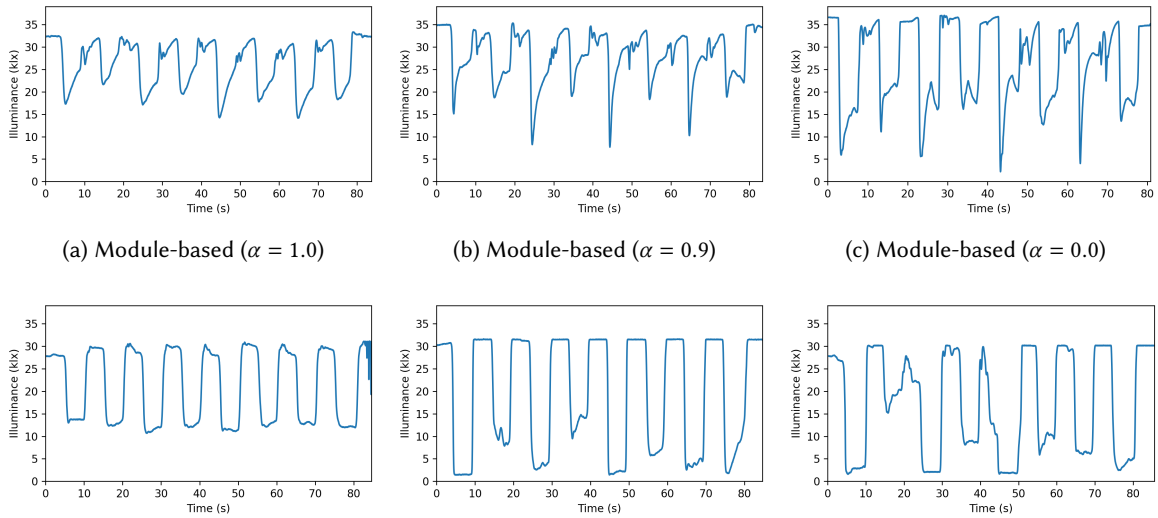


(a) Module-based ($\alpha = 1.0$) (b) Module-based ($\alpha = 0.9$) (c) Module-based ($\alpha = 0.0$)

(d) Conventional OR Light (Pos 1) (e) Conventional OR Light (Pos 2) (f) Conventional OR Light (Pos 3)

Fig. 10. Illuminance on the surface of the white plastic plate during the first experiment, averaged over all 24 x 24 pixels and plotted over time. It is visible how the subjects (who moved according to the pattern illustrated in Figure 9) bent forward and backward eight times, each time leading to a decrease and again to an increase of the illuminance on the white plate. In the case of the autonomous module-based lighting system, it can be seen that immediately after bending forward, the light intensities are adjusted so that the illumination becomes brighter again, whereas, with the conventional OR light, the brightness remains constantly low while people bend forward.

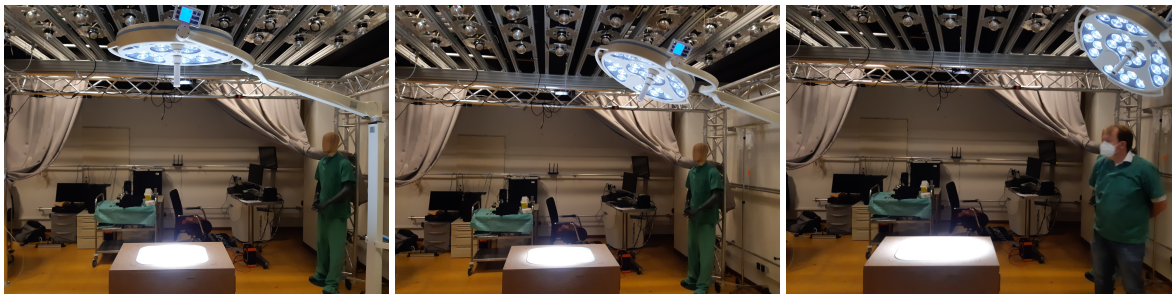

(a) Position 1 (b) Position 2 (c) Position 3

Fig. 11. Positioning and alignment of the conventional OR light during experiment 1.

In the first experiment, which was performed to examine the active shadow avoidance by our intensity optimization, four people of different heights were standing around the wooden box and moved according to a pattern illustrated in Figure 9. This pattern was repeated for six lighting conditions, three conditions using the new module-based lighting system with (1) $\alpha = 0.0$, (2) $\alpha = 0.9$ and (3) $\alpha = 1.0$, and three conditions using a

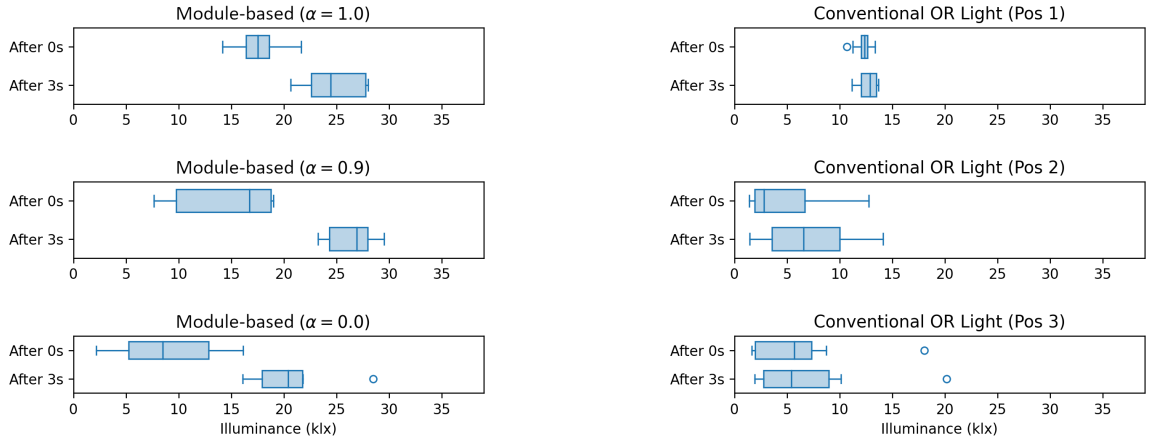


Fig. 12. Illuminance on the surface of the white plastic sheet during the first experiment, (1) immediately after the subjects have bent over, and (2) three seconds after the subjects have bent over. With the autonomous module-based lighting system, a significant increase in illuminance is perceptible after three seconds due to the intensity optimization, while the intensity remains approximately the same with the conventional OR light.

conventional OR light at three different positions, namely (Pos 1) directly over the table, (Pos 2) moved somewhat to the side and (Pos 3) moved further to the side (see Figure 11).

The results, which are plotted temporally in Figure 10 and plotted as box plots in Figure 12, clearly show that the intensity optimization of the lighting system greatly reduces shadows even with four people leaning over the site. In the case of the autonomous lighting system, there is a short, intense drop in illumination when the persons lean forward, but this is immediately compensated for by the intensity optimization, whereas there is no compensation in the case of the conventional OR light (see Figure 10). In the case of the autonomous lighting system, it is also noticeable that at $\alpha = 1.0$ – i.e. when as many light modules as possible are used at the same time – there is a significantly smaller drop in illuminance, which is compensated more slowly. In contrast, the decrease of illuminance is significantly higher when using fewer light modules (i.e. , $\alpha = 0.9$ or $\alpha = 0.0$) and the readjustment is correspondingly faster. It is also noticeable that with the autonomous lighting system at $\alpha = 0.0$ after a drop in illuminance, there is always a rapid compensation, but shortly afterward a slight drop occurs again – this might be because at $\alpha = 0.0$ as few lights as possible should be used at the same time, but in this scenario with four people, hardly any light module alone can illuminate the entire white area without shadows. The peak might be caused by the change of the light modules, in which in the transition phase several light modules shine at the same time for a short time, which together can achieve better illumination.

In summary, even in such a challenging case with four people fully bending over the site at the same time, almost touching their heads, a significant improvement in illumination is possible with the help of the autonomous module-based lighting system.

### 6.3 Experiment 2: Passive Shadow Reduction

The second experiment was designed to investigate the ability of passive shadow reduction of near objects: While our intensity optimization only considers objects with a minimum distance $r$ around the surgical site (we used $r = 0.3$ m), it is expected that the shadow behavior within that distance will also be significantly different

compared to conventional OR lights for near objects like hands and medical instruments, simply due to the large number of light modules distributed over a large area at the ceiling.

We asked 8 subjects (3 male, 5 female, all between 18 and 30 years old) to work with Lego bricks, which would create shadows cast by their hands over the plastic plate (see Figure 13). The task was to create nine identical lego shapes consisting of four distinctly-colored bricks on the plastic plate. For each Lego shape, a cornerstone was given; the participants had to attached three other Lego bricks in a specific orientation. These Lego bricks had to be found in a box full of Lego. Subjects were instructed not to lift the cornerstones. In the case of the conventional OR light, we placed it slightly to the side of the test subjects, opposite the Lego box, so that it was not occluded by the subject's head or body throughout the trial — manual readjustment by the test subject was thus not necessary and not performed. All participants repeated the task for all four lighting conditions in random order.

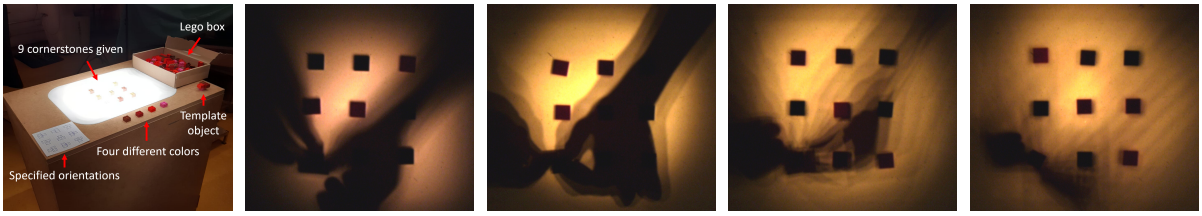


(a) Setup (b) Conventional OR light (c) Module-based ($\alpha = 0.0$) (d) Module-based ($\alpha = 0.9$) (e) Module-based ($\alpha = 1.0$)

Fig. 13. Experiment 2: Different lighting conditions in a comparable situation recorded by the camera placed in the box. This diagram shows how the parameter $\alpha$ affects the characteristics of shadows near the surgical site, such as those cast by hands, within an autonomous lighting system. The system can be adjusted from using a few very bright lights ($\alpha = 0.0$) to using many dimmer lights ($\alpha = 1.0$).

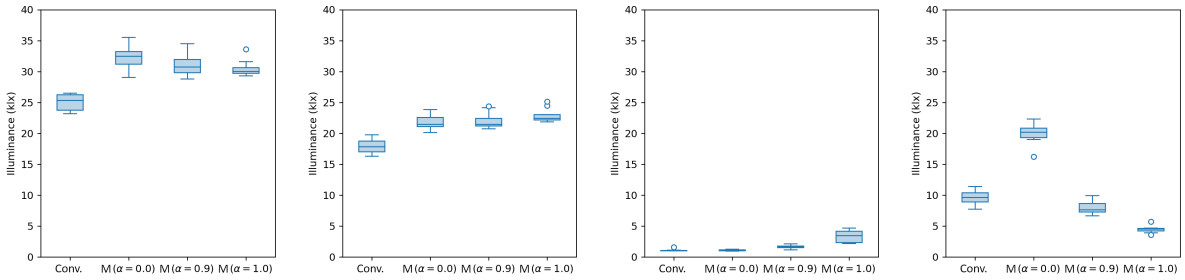


(a) Maximal brightness (b) Average brightness (c) Minimal brightness (d) Maximal delta

Fig. 14. For each sensor, the maximal brightness (a), average brightness (b), minimal brightness (c) and maximal delta (to the previous frame) were calculated individually and then averaged over all 576 virtual sensors, shown as box plots of all trials (n=8) for every lighting condition.

We plotted the maximal, average, and minimal brightness of the illumination systems in Figure 14, averaged over all 576 virtual sensors (i.e. over the illuminated area). While there are only little differences in brightness relative to each other for the maximum and average brightness, it is noticeable in the minimum brightness that the module-based lighting system with $\alpha = 0.9$ (approximately 11 simultaneously shining light modules), but especially with $\alpha = 1.0$ (up to 48 simultaneous shining light modules, as some light modules could not be aligned

with the site due to the limited motor angle), produces significantly higher minimum brightness (see Figure 14c), indicating that these systems are better at compensating for total shadowing. This means that the most poorly illuminated situations are significantly brighter with our module-based lighting system with $\alpha = 1.0$, giving surgeons better visibility in these situations. Figure 15 shows that this applies not only to border areas but also to the focus area in between the Lego bricks.

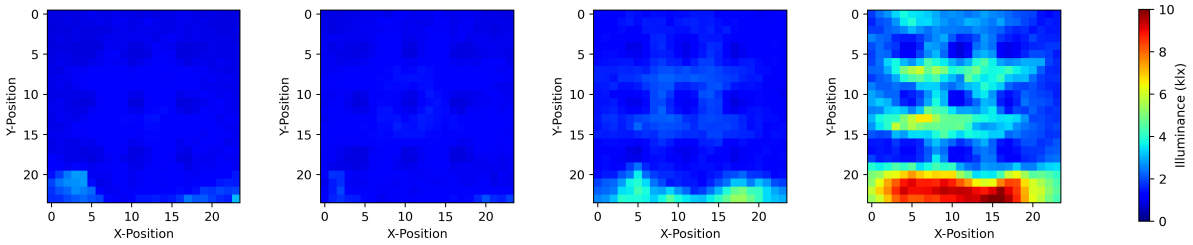


(a) Conventional OR light (b) Module-based ($\alpha = 0.0$) (c) Module-based ($\alpha = 0.9$) (d) Module-based ($\alpha = 1.0$)

Fig. 15. Minimal brightnesses over time per sensor averaged over trials (n=8). It can be seen that in the case of $a \geq 0.9$, noticeably higher minimum intensities are achieved, which means that it becomes significantly less dark in the entire working area over the course of the entire trial. Note that the 3 x 3 dark spots come from the placed Lego bricks blocking the light and that this is not caused by the lighting systems.

The maximum delta (shown in Figure 14d) describes the maximum brightness changes between two adjacent frames. Assuming that shadow movement cast by our test subjects are on average equally fast, these characterize the hardness of moving shadows. In Figure 14d and Figure 16 it is visible that the shadow hardness in the module-based system strongly depends on the number of light modules used simultaneously: When using only two light modules in the module-based lighting system, there is a doubling of brightness changes compared to a conventional OR light – means that the shadows are considerably harder. However, with $\alpha = 0.9$ ($\approx 11$ light modules) the shadow hardness is slightly lower compared to the conventional OR light and when using $\alpha = 1.0$ (up to 48 light modules) it is halved compared to the conventional OR light. Finally, shadows are much harder when using $\alpha = 0.0$ (not more than two light modules).

The experiment showed that the module-based lighting system can compensate for (a) total shadowing significantly better as well as (b) produce softer shadows compared to the conventional OR light (Dr. Mach LED 3) in case of shadows by *hands* and *medical instruments*, especially when using all light modules simultaneously. However, this strongly depends on the number of light modules used at the same time – if this number is too low (e.g. , when using $\alpha = 0.0$, which corresponds to two light modules used simultaneously), the module-based system may also perform significantly worse regarding the hardness of shadows compared to the conventional OR lights used in our experiment. So finally, in terms of shadowing, the system should be operated with as many light modules as possible at the same time – then it is clearly superior to the conventional OR light.

## 7 Semi-Structured Interviews

We conducted four semi-structured interviews with actively practicing surgeons at Pius Hospital Oldenburg in Germany to obtain first feedback on the light characteristics and applicability of the autonomous module-based lighting system. We used the results to select appropriate questions in the following comparative study presented in Section 8.

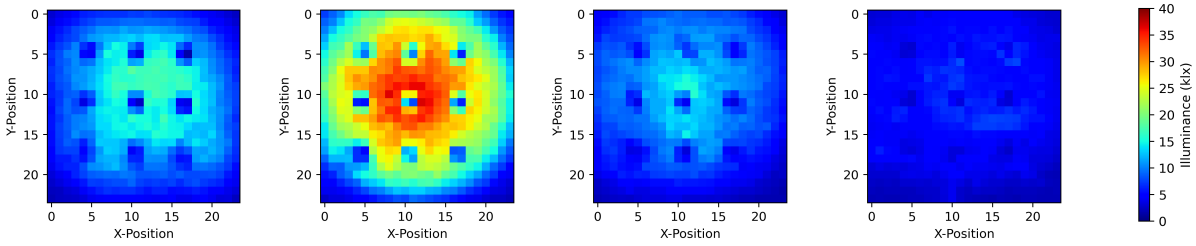


(a) Conventional OR light (b) Module-based ($\alpha = 0.0$) (c) Module-based ($\alpha = 0.9$) (d) Module-based ($\alpha = 1.0$)

Fig. 16. Maximal Delta: The maximum change in brightness in two consecutive frames throughout the experiment per sensor averaged over trials (n=8), which indicates the hardness of moving shadows. It is clearly visible that depending on the choice of parameters, the autonomous module-based surgical lighting system can create much softer shadows than the conventional OR light when using $\alpha = 0.9$ or $\alpha = 1.0$. Note that the 3 x 3 dark spots come from the placed Lego bricks which are blocking the light, and that this is not caused by the lighting systems.

## 7.1 Setup and Procedure

In each interview, we presented our prototype on an artificially prepared surgical site consisting of red cloths in a Styrofoam manikin placed on an operating table and covered with surgical drapes (see Figure 18). This surgical site was 21 cm x 12 cm in size and 10cm deep at each of its longest points. During the interview, the surgeon could suture a wound of a banana or orange using surgical suture material and instruments. At the beginning of each interview, we asked the surgeon to describe the light of the prototype with its characteristics using all light modules simultaneously. We then asked the surgeons about the brightness, shadow cast, reaction speed, reflections and glare of the different conditions and, by request, varied the parameters of brightness, number of simultaneously active light modules (in three steps, as done in Section 6) and reaction speed of the prototype. In addition, a mobile conventional OR light with a single lighting unit, the Dr. Mach LED 3, was available for comparison (as it was in Section 6).

Fig. 17. Experimental setup of the semi-structured interviews.

## 7.2 Results

The illumination of the site was perceived as very homogeneous by the participating surgeons when using the prototype with all light modules simultaneously. The area illuminated by the prototype was described as larger and the light as having a softer fade out compared to the previous experience of conventional OR lights resulting in lower contrast. With regard to their satisfaction with the light, it did not matter whether the surgeons were alone at the operating table or surrounded by two other people (see Figure 17). Reducing the number of simultaneously active light modules tended to reduce satisfaction in terms of illumination, particularly with as few light modules as possible.

With regard to shadows, it was noted that there were hardly any shadows present using all light modules which was described as much less than they were used to from conventional OR lights. In particular, hand and instrument shadows were perceived by surgeons as marginal and barely existent. We also asked surgeons in particular about the somewhat blocky shape of the shadows, but it was not found to be a bother of any kind. Shadows through bodies and heads were not noticed at all. After we reduced the number of simultaneously active lights ($\alpha = 0.9$), there was a bit more shadowing by hands and instruments perceived, which was still judged to be more satisfactory than the conventional OR lights. However, as soon as the number of simultaneously active lights was further reduced to 2-4 light modules, it was noted that head and body shadows became visible during movements, even if they were fully compensated within a few seconds. Hand and instrument shadows were perceived as much more visible when using as few light modules as possible.

The permanent automatic readjustment of the brightness of individual light modules was hardly or not at all noticeable to the surgeons in the illuminated area with $\alpha = 0.9$ or higher. We also asked the surgeons to take a look at the ceiling and pay attention to the changes in brightness – some surgeons were surprised that there were quite a lot of intensity changes in the lights which were not visible in the illumination of the surgical site. The set reaction speed was found to be very pleasant. When we significantly increased the reaction speed for some participating surgeons as a test, the autonomous intensity readjustment became visible in the light field and tended to be judged as more disturbing.

With regard to the topic of whether reflections on medical instruments are a major problem in the operating room, there were basically very different opinions from the participating surgeons. Some participants perceived reflections using the prototype as well as using the conventional OR light, while others did not. When reflections were perceived, they tended to be perceived as more disturbing when using the conventional OR light than using the prototype, especially when many light modules were used. One of the reasons for the latter could be that the light in the prototype is distributed over a large area using a large number of light modules, which means that less light comes from the same direction.

As another important point, surgeons noted that the prototype may not be suitable for all types of surgery, especially those in which the light must enter the body at a very oblique angle. After all, the light modules are fixed to the ceiling and are not movable. Examples given were thyroid, biliary, diaphragmatic, stoma, and rectal surgeries (e.g. , lithotomy positioning). To solve the problem, it was suggested to arrange the light modules parabolically on the ceiling, to attach some light modules to the walls as well, or to have a mobile conventional OR light available as a fallback for such cases. Furthermore, some surgeons noticed a loud, high-pitched buzzing noise by the prototype, which two participants found somewhat disturbing to very annoying. However, this is a technical problem specific to the prototype, independent of the lighting concept, although this may have had a slight negative impact on the scoring of the prototype in the comparative study in Section 8, more on this later.

Regarding the setup, we received the suggestion that the additional persons present might wear typical surgical clothing (instead of partly very dark clothing) in order to better reflect possible glare from the light on clothing – we considered this in the comparative study presented in Section 8. However, the setup was found to be suitable overall for comparing the illumination by the prototype with the illumination by a conventional OR light and

the size of the mimicked surgical site was found to be comparable to many typical abdominal surgeries. Finally, the surgeons found the actual prototype to be very promising after testing and seemed impressed with the illumination compared to conventional OR lights.

## 8 Comparative Study

We conducted a laboratory comparative study comparing the prototype of the autonomous module-based lighting system with a conventional OR light (Dr. Mach LED 3), where we had surgeons compare different characteristics of the lighting systems, and the surgeons were asked to give a preference of the lighting system at the end. The comparison study was conducted including 11 actively practicing surgeons from Pius Hospital Oldenburg, Germany.

### 8.1 Setup and Procedure

The comparative study was performed with two conditions of the autonomous module-based illumination system (i.e. , with $\alpha = 1.0$ and $\alpha = 0.9$) and with one condition of the mobile conventional OR light (DR. Mach LED 3), which were performed in randomized order. The brightness of the autonomous illumination system was chosen in such a way that an illuminance of 100 klx was approximately achieved in the center of the illuminated area, as this value was judged to be realistic by the surgeons in the previous semi-structured interviews. The number of simultaneously active light modules, which is determined by the parameter $\alpha$, also depends on the brightness, since each light module can only provide a limited brightness. While with $\alpha = 1.0$ still all possible light modules were used (which corresponds to 48 light modules, as some light modules could not be aligned with the site due to the limited motor angle), with $\alpha = 0.9$ about 19 simultaneously active light modules were used – here $\alpha = 0.9$ thus corresponds to a higher number of light modules than in the measurements in Section 6, where a lower brightness was used.

In each of the three lighting conditions, surgeons were required to find and extract nine tacks from an orange and suture two incisions without moving the orange (see Figure 18). If the orange was accidentally moved by the surgeon, it was put back by the assisting experimenter when the tacks were put away or after a suture was completed.

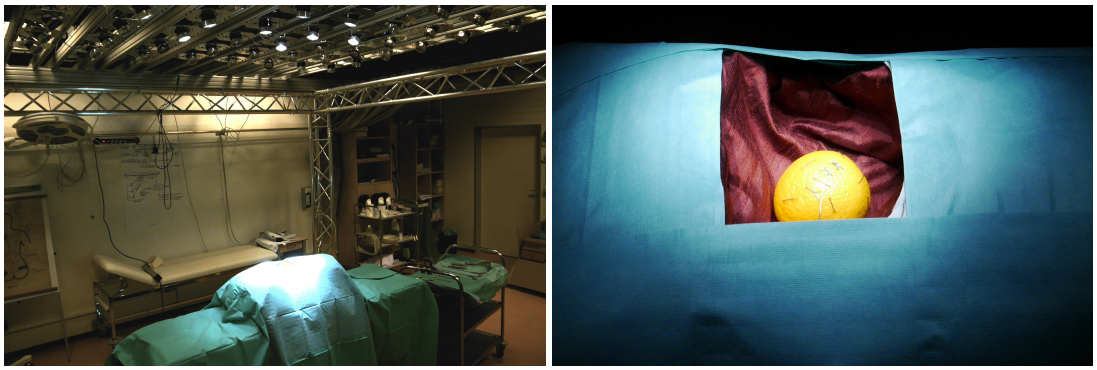

(a) Experimental Setup (b) Surgical Site

Fig. 18. Experimental setup in the comparison study.

The tacks were randomly placed all over the upper hemisphere of the orange to provoke a movement of the head over the site. To reduce a learning effect when looking for the tacks, their positions differed in the experimental conditions. The incisions, on the other hand, were identical in different conditions: The first incision was within easy reach of the surgeon, and the second facing away from the surgeon, again to provoke the surgeon to lean forward. In all trials, two research assistants stood opposite the surgeon in front of the OR table and had the suturing techniques performed explained to them in order to create a scenario closer to the operating room in terms of illumination, but also to direct the focus of the subjects to something other than the light.

After each of the three experimental conditions, the surgeon completed a questionnaire regarding the illumination properties of the surgical site. After all three conditions, the surgeons were asked to complete a last questionnaire in which the surgeon was asked to indicate a preference for lighting systems.

## 8.2 Questionnaires

We designed two questionnaires: The first questionnaire was answered three times by the surgeon, each time after a lighting condition was performed, and contained questions regarding the lighting properties. The second questionnaire was answered by the surgeon after all three conditions were performed and asked for a preference for lighting conditions.

The first questionnaire is based on the LiTG questionnaire [39] but was adapted to the situation of the illumination of a surgical site, especially with regard to shadowing. The answers were each given on a seven-point Likert scale. Another option would be the use of VERAM, which is a validated method for evaluating visual ergonomics in workplaces [47][13] and has also been used in an adapted version to evaluate the requirements of surgical lighting [14]. However, it did not seem to be sufficiently focused on the analysis of shadows. The focus of the questionnaire seemed to be more on exposure over a longer period of time (e.g. , regarding glare due to excessive brightness over the entire period of surgery). In our study, the test subjects were only available for a short period of time, and the actual prototype is understandably not allowed to be used in the context of real surgeries due to laws so no field study was feasible that could measure fatigue symptoms over a longer period of time. In the second questionnaire, the surgeons had to give a preference from 1 to 3, with 1 indicating the most preferred lighting system and 3 indicating the least preferred lighting system. We repeated the question with respect to three contexts:

(a) The first question was related to the laboratory experiment with the orange.
(b) The second question was to state what system the surgeons would most likely use for real surgeries with a comparable surgical site.
(c) The third question was an extension of the second question, where the preference was not only to be given to the three conditions but in addition, a fourth lighting system was available for selection: the ceiling mounted OR lights with two or three light units, which surgeons are familiar with from the OR rooms where they perform their daily work. Here, surgeons had to indicate their preferences from (1) the most preferred condition to (4) the least preferred condition.

## 8.3 Results

Our results of the questionnaires regarding the illumination properties, which were completed after each condition, are shown in Figure 19 and in Table 3, while the results of the final questionnaire regard the preference are shown in Figure 20.

In the evaluation of the properties of the light, on which the surgeons were asked after performing each condition, there were some significant differences between both autonomous module-based OR lighting conditions and the conventional OR light: With respect to both (1) illumination in general, (2) distribution of light, (3) removal of shadow, (4) shadow properties in general, (5) satisfaction, and (6) suitability of the lighting system, both

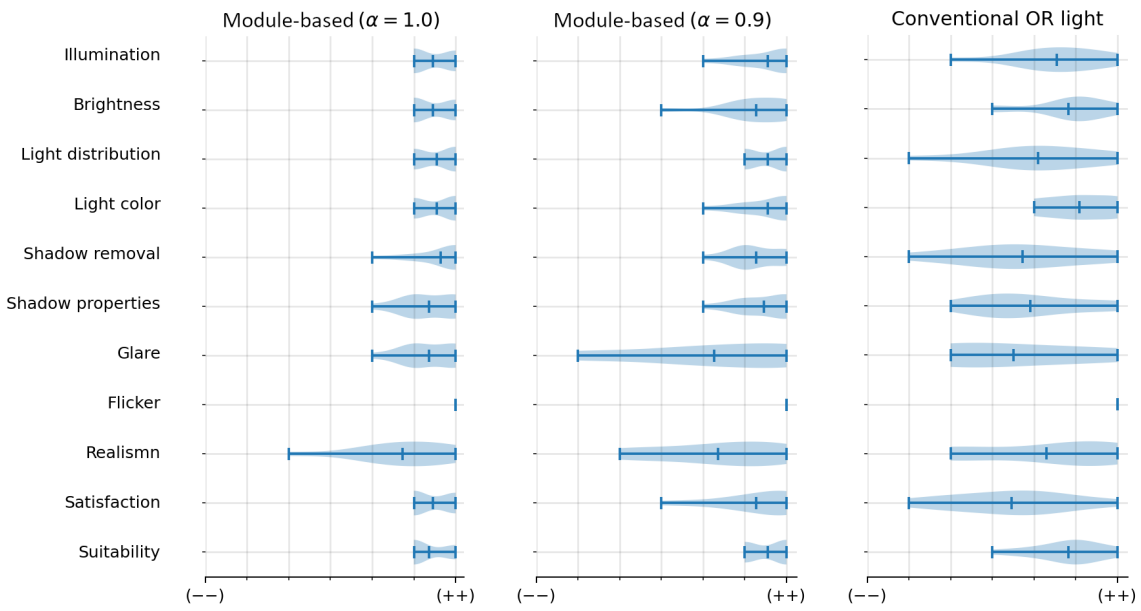


Fig. 19. Rating of various properties of the light given by the surgeons after each condition was conducted ($n = 11$). The seven-point scale was labeled with "very dissatisfied" (--) to "very satisfied" (++) on the questionnaires, with the exception of (1) glare and flicker, where we use ”very distracting" (--) to "not distracting" (++), and (2) suitability which was ”very unsuitable” (--) to ”very suitable” (++).

conditions of the autonomous lighting system performed significantly ($p \leq 0.05$) better than the conventional OR light. In one case – namely, the removal of the shadow – the $\alpha = 1.0$ variant of the autonomous lighting system performed better than the $\alpha = 0.9$ variant, which is consistent with the greater number of simultaneously shining light modules. In contrast, the conventional OR light did not perform better than any of the autonomous lighting system conditions on any light property.

Regarding satisfaction with brightness, the autonomous lighting system with $\alpha = 1.0$ also performed boundary-significantly better than the conventional OR light. Although there is no significant difference regarding the brightness between the autonomous conditions with $\alpha = 1.0$ and $\alpha = 0.9$, it is noticeable that $\alpha = 1.0$ might tend to be a little better than $\alpha = 0.9$. In particular, for *Glare* there is a tendency that **M** ($\alpha = 1.0$) might be better than **M** ($\alpha = 0.9$) – however, it should be noted that *Glare* depends very much on the brightness setting, which we have already chosen quite high with 100 klx, and, due to minor inaccuracies of the calibrations in the actual prototype, the prototype produces a slightly more focused and thus slightly brighter light than when using many light modules, as visible e.g. in Figure 14a. One property that stands out a little is *Realism* – here, surgeons were asked to judge how realistic the presented scenario was in terms of illuminating a situs compared to a real OR. Here, our expectation was that there would be no significant difference between the conditions.

The results of the final questionnaire show quite clearly that the autonomous module-based surgical lighting system is preferred compared to conventional OR lights. The module-based lighting system was by far the most preferred lighting system with $\alpha = 1.0$ and the second most preferred lighting system with $\alpha = 0.9$. In particular, it should be noted that in all scenario (a), (b), and (c) the conventional OR lights with a single lighting unit was

Table 3. Mean and standard deviation of the properties asked about, as well as p-values of a one-way ANOVA and p-values of paired t-tests. Condition **M** refers to the autonomous module-based lighting system and condition **C** to the conventional OR light (Dr. Mach LED 3). The seven-point Likert scale was numbered from 1 to 7 in the evaluation. The sample size was generally n=11. However, there were deviations for individual properties due to non-given responses, which are: Glare with $n = (7, 8, 4)$ for the individual conditions, Flicker with $n = (2, 2, 1)$ and Realism with $n = (11, 11, 10)$. Since we used the paired t-test, we did not evaluate for *Glare* and *Flicker* due to the small $n$ and used n=10 in all conditions for realism. P-values that were less than 0.05 are assumed to be significant and are thus highlighted in bold.

| | **Mean (SD)** | | | **ANOVA** | **Paired t-test** | | |
|---|---|---|---|---|---|---|---|
| **Property** | **M ($\alpha$ = 1.0)** | **M ($\alpha$ = 0.9)** | **C** | | **M(1.0) – M(0.9)** | **M(1.0) – C** | **M(0.9) – C** |
| Illumination | 6.45 (0.5) | 6.55 (0.66) | 5.55 (1.08) | **0.013** | 0.588 | **0.005** | **0.019** |
| Brightness | 6.45 (0.5) | 6.27 (0.86) | 5.82 (0.94) | 0.195 | 0.441 | **0.046** | 0.296 |
| Light distribution | 6.55 (0.5) | 6.55 (0.5) | 5.09 (1.38) | **0.001** | 1.0 | **0.002** | **0.007** |
| Light color | 6.55 (0.5) | 6.55 (0.66) | 6.09 (0.79) | 0.222 | 1.0 | 0.138 | 0.138 |
| Shadow removal | 6.64 (0.64) | 6.27 (0.62) | 4.73 (1.48) | **0.0004** | **0.038** | **0.002** | **0.005** |
| Shadow properties | 6.36 (0.64) | 6.45 (0.66) | 4.91 (1.24) | **0.0006** | 0.588 | **0.001** | **0.001** |
| Glare | 6.0 (0.53) | 4.62 (1.8) | 4.5 (1.66) | — | — | — | — |
| Flicker | 7.0 (0.0) | 7.0 (0.0) | 7.0 (0.0) | — | — | — | — |
| Realismn | 5.73 (1.14) | 5.36 (1.43) | 5.3 (1.62) | 0.770 | 0.269 | 0.468 | 0.800 |
| Satisfaction | 6.45 (0.5) | 6.27 (0.96) | 4.45 (1.37) | **0.0001** | 0.441 | **0.0009** | **0.005** |
| Suitability | 6.36 (0.48) | 6.55 (0.5) | 5.82 (0.83) | **0.038** | 0.167 | **0.025** | **0.012** |

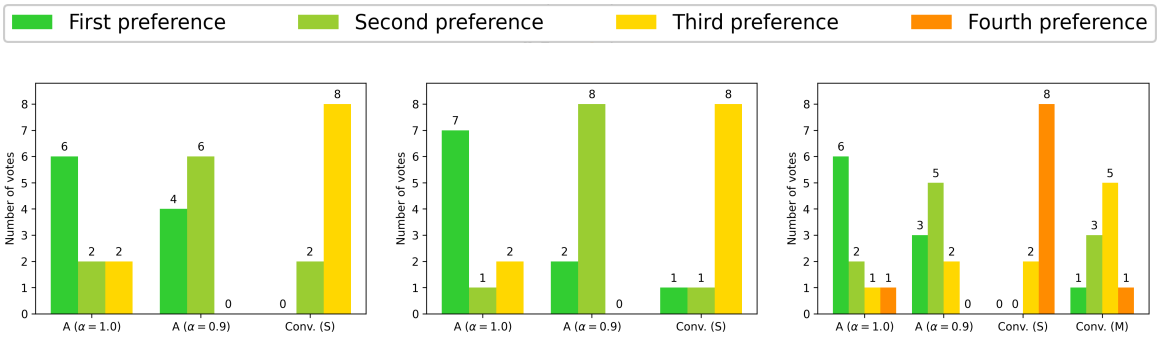


(a) Experimental Setup (b) Real surgery (estimate) (c) Real surgery (estimate)

Fig. 20. Preference of lighting systems by surgeons after conducting experiments. Here, 'M ($\alpha$ = 1.0)' and 'M ($\alpha$ = 0.9) refer to the autonomous module-based illumination system with the respective configuration, 'Conv (S)' refers to the actual used conventional OR light (Dr. Mach LED 3) with only a single lighting unit, and 'Conv (M)' refers to the conventional OR lights known by the surgeons in typical surgery rooms which have multiple (usually two or three) lighting units. One surgeon's questionnaire was excluded from the preference evaluation due to incorrect completion (there, M ($\alpha$ = 1.0) was checked as the presumed preferred system for every question, without indicating a graded preference of all systems), resulting in $n$ = 10.

never chosen as the most preferred system, while the conventional OR lights with multiple lighting units that the surgeons were familiar with was only the most preferred lighting system by only one person. However, it is striking that the prototype with $\alpha = 1.0$ was chosen in rare cases as the least preferred system in scenarios (1) and (2). This was justified by the subjects in the comments with the loud beeping, which was already addressed in section 7.2 and thus may have less to do with the lighting concept and the illumination itself. Finally, the results strongly suggest that for comparable surgical sites, the novel autonomous module-based surgical lighting system provides illumination of the surgical site that is perceived by surgeons as significantly better.

# 9 Conclusion

## 9.1 Summary and Results

We have presented a new lighting concept for operating rooms consisting of a large number of small ceiling-mounted light modules whose intensity and orientation are autonomously controlled by a central computer. For this system, we presented (1) an optimization procedure for determining optimal positions for light modules on the ceiling and (2) an algorithm for controlling and determining optimal intensities of the individual light modules during surgery. We have implemented this lighting concept as a real prototype at a German hospital and evaluated it with respect to its illumination properties. Our results show that the autonomous, module-based lighting concept is capable of significantly reducing shadows both actively and passively. This lighting concept performed significantly better in essential illumination properties such as shadowing and light distribution, but also satisfaction and suitability in a study with eleven actively practicing surgeons when used in the abdominal area. Moreover,the autonomous module-based lighting system was clearly preferred by these surgeons compared to conventional OR lights.

## 9.2 Limitations

While the system can be used for a variety of surgical procedures, particularly in the abdominal area (e.g., cholecystectomy, pancreatic resection, liver resection), there are specific operations (e.g., those utilizing the lithotomy position) where light must not primarily enter from above but rather from the side into the surgical wound. In these cases, our lighting concept, which relies solely on ceiling-mounted light modules, is not feasible if the angle of light entry is too acute. It might be necessary to place special light modules on the walls or add conventional OR lights in these situations.

## 9.3 Future Work

In future work, a number of avenues can be addressed: For example, optimization of light positions on OR recordings made in different OR rooms with non-abdominal surgeries exclusively might be very useful to obtain information about the generalizability of light module positions across multiple rooms and surgery types. Instead of using conventional OR lights when performing these depth recordings, it might be beneficial to use the novel autonomous module-based lighting system, since the movement of OR personnel might be different if they don't have to worry about shadows. In addition, the intensity optimization procedure can be extended to multiple sample points in the surgical site and tested for possible improvements — here the use of heuristic optimization algorithms, such as the one we used for position optimization, might be appropriate. Last but not least, a field study on the illumination concept in productive use should be performed once a suitable prototype has received approval for use in real surgeries.

## Acknowledgements and Notes

This work was partially supported by BMBF grant 13GW0264D. A positive vote of the Ethics Committee was received in advance for all studies conducted with external subjects.

## References


[1] William C. Beck. 1981. Operating room illumination: the current state of the art. *Bull Am Coll Surg* 66, 5 (May 1981), 10–15.

[2] Francesco Biscani and Dario Izzo. 2020. A parallel global multiobjective framework for optimization: pagmo. *Journal of Open Source Software* 5, 53 (2020), 2338. https://doi.org/10.21105/joss.02338

[3] F. Borie, M. Mathonnet, A. Deleuze, B. Millat, J-F Gravié, H. Johanet, J-P Lesage, and J. Gugenheim. 2018. Risk management for surgical energy-driven devices used in the operating room. *Journal of Visceral Surgery* 155, 4 (Sep 2018), 259–264. https://doi.org/10.1016/j.jviscsurg.2017.12.003

[4] Jarryd Michiel Burger. 2019. *Automated Surgical Light Positioning System Using Thermal-imaging and Optical Techniques.* Master's thesis. Stellenbosch University. https://scholar.sun.ac.za/bitstream/10019.1/106092/3/burger_automated_2019.pdf

[5] Timur Cetin, Andre Mühlenbrock, Gabriel Zachmann, Verena Weber, Dirk Weyhe, and Verena Uslar. 2023. A virtual reality simulation of a novel way to illuminate the surgical field – A feasibility study on the use of automated lighting systems in the operating theatre. *Frontiers in Surgery* 10 (2023). https://doi.org/10.3389/fsurg.2023.1055053

[6] Dong-Geol Choi, Byung-Ju Yi, and Whee-kuk Kim. 2007. Automation of Surgical Illumination System Using Robot and Ultrasonic Sensor. In *2007 International Conference on Mechatronics and Automation.* 1062–1066. https://doi.org/10.1109/ICMA.2007.4303695

[7] Thomas H. Cormen, Charles E. Leiserson, Ronald L. Rivest, and Clifford Stein. 2009. *Introduction to Algorithms, 3rd Edition.* MIT Press. http://mitpress.mit.edu/books/introduction-algorithms

[8] Jahnavi Curlin and Charles K. Herman. 2020. Current State of Surgical Lighting. *Surg J (N Y)* 6, 2 (June 2020), e87–e97. https://doi.org/10.1055/s-0040-1710529

[9] Armin Dietz, Stephan Schröder, Andreas Pösch, Klaus Frank, and Eduard Reithmeier. 2016. Contactless Surgery Light Control based on 3D Gesture Recognition. In *GCAI 2016. 2nd Global Conference on Artificial Intelligence (EPiC Series in Computing, Vol. 41)*, Christoph Benzmüller, Geoff Sutcliffe, and Raul Rojas (Eds.). EasyChair, 138–146. https://doi.org/10.29007/zmz9

[10] Robert Elfring, Frank Franz, Hanno Kretshmann, and Stefan Schlighting. 2016. Method for improving the illumination of an illumination region from an illumination device. https://patents.google.com/patent/US20160174336 US Patent 2016/0174336A1.

[11] Saber M. Elsayed, Ruhul A. Sarker, and Daryl L. Essam. 2011. Differential evolution with multiple strategies for solving CEC2011 real-world numerical optimization problems. *2011 IEEE Congress of Evolutionary Computation (CEC)* (2011), 1041–1048.

[12] International Electrotechnical Commission et al. 2013. *Medical electrical equipment - Part 2-41: Particular requirements for the basic safety and essential performance of surgical luminaires and luminaires for diagnosis.* Technical Report IEC 60601-2-41:2009+AMD1:2013.

[13] Marina Heiden, Camilla Zetterberg, Per Lindberg, Per Nylén, and Hillevi Hemphälä. 2019. Validity of a computer-based risk assessment method for visual ergonomics. *International Journal of Industrial Ergonomics* 72 (2019), 180–187. https://doi.org/10.1016/j.ergon.2019.05.006

[14] H. Hemphälä, W. Osterhaus, P.A. Larsson, J. Borell, and P. Nylén. 2020. Towards better lighting recommendations for open surgery. *Lighting Research & Technology* 52, 7 (2020), 856–882. https://doi.org/10.1177/1477153520903355 arXiv:https://doi.org/10.1177/1477153520903355

[15] C. Hensman, G. B. Hanna, T. Drew, H. Moseley, and A. Cuschieri. 1998. Total radiated power, infrared output, and heat generation by cold light sources at the distal end of endoscopes and fiber optic bundle of light cables. *Surgical Endoscopy* 12, 4 (01 Apr 1998), 335–337. https://doi.org/10.1007/s004649900665

[16] A. Katharine Hindle, Fred Brody, Vernon Hopkins, Greg Rosales, Florencia Gonzalez, and Arnold Schwartz. 2009. Thermal injury secondary to laparoscopic fiber-optic cables. *Surgical Endoscopy* 23, 8 (Aug 2009), 1720–1723. https://doi.org/10.1007/s00464-008-0219-z

[17] John H. Holland. 1992. *Adaptation in Natural and Artificial Systems: An Introductory Analysis with Applications to Biology, Control and Artificial Intelligence.* MIT Press, Cambridge, MA, USA.

[18] Jessita Joseph and D.S. Divya. 2018. Hand Gesture Interface for Smart Operation Theatre Lighting. *International Journal of Engineering & Technology* 7, 2.25 (2018), 20–23. https://doi.org/10.14419/ijet.v7i2.25.12358

[19] Dervis Karaboga and Bahriye Basturk. 2007. A powerful and efficient algorithm for numerical function optimization: artificial bee colony (ABC) algorithm. *Journal of Global Optimization* 39, 3 (01 Nov 2007), 459–471. https://doi.org/10.1007/s10898-007-9149-x

[20] James Kennedy and Russell Eberhart. 1995. Particle swarm optimization. In *Proceedings of ICNN'95 - International Conference on Neural Networks*, Vol. 4. 1942–1948 vol.4. https://doi.org/10.1109/ICNN.1995.488968

[21] S. Kirkpatrick, C.D. Gelatt, Jr., and M.P. Vecchi. 1983. Optimization by simulated annealing. *Science* 220, 4598 (May 1983), 671–680.

[22] Arjan J. Knulst, Jeroen Kunst, and Jenny Dankelman. 2019. Lightfield adaptable surgical luminaire concept. *J Med Eng Technol* 43, 6 (Oct. 2019), 378–386. https://doi.org/10.1080/03091902.2019.1681529

[23] Arjan J. Knulst, Rik Mooijweer, Frank W. Jansen, Laurents P.S. Stassen, and Jenny Dankelman. 2010. Indicating shortcomings in surgical lighting systems. *Minim Invasive Ther Allied Technol* 20, 5 (Nov. 2010), 267–275. https://doi.org/10.3109/13645706.2010.534169

[24] Arjan J. Knulst, Jesse van Dongen, Marco W. M. Groenewegen, Elisabeth D. Kaptein, and Jenny Dankelman. 2011. The Effect of Shadows on Performing Stereo visual Pointing Tasks: Is Shadow-Free Open Surgery Ideal? *LEUKOS* 8, 2 (2011), 111–122. https://doi.org/10.1582/LEUKOS.2011.08.02.002

[25] Marek Kowalski, Jacek Naruniec, and Michal Daniluk. 2015. Livescan3D: A Fast and Inexpensive 3D Data Acquisition System for Multiple Kinect v2 Sensors. In *2015 International Conference on 3D Vision*. 318–325. https://doi.org/10.1109/3DV.2015.43

[26] Andreas Kunz, Luzius Brogli, and Ali Alavi. 2016. Interference measurement of kinect for xbox one. In *Proceedings of the 22nd ACM Conference on Virtual Reality Software and Technology* (Munich, Germany) *(VRST '16)*. Association for Computing Machinery, New York, NY, USA, 345–346. https://doi.org/10.1145/2993369.2996329

[27] Ulrich Matern and Sonja Koneczny. 2007. Safety, hazards and ergonomics in the operating room. 21, 11 (01 November 2007), 1965–1969. https://doi.org/10.1007/s00464-007-9396-4

[28] Seyedali Mirjalili, Seyed Mohammad Mirjalili, and Andrew Lewis. 2014. Grey Wolf Optimizer. *Advances in Engineering Software* 69 (2014), 46–61. https://doi.org/10.1016/j.advengsoft.2013.12.007

[29] Andre Mühlenbrock, Roland Fischer, Christoph Schröder-Dering, René Weller, and Gabriel Zachmann. 2022. Fast, accurate and robust registration of multiple depth sensors without need for RGB and IR images. *The Visual Computer* (17 May 2022). https://doi.org/10.1007/s00371-022-02505-2

[30] Andre Mühlenbrock, René Weller, and Gabriel Zachmann. 2023. Optimizing the Illumination of a Surgical Site in New Autonomous Module-based Surgical Lighting Systems. In *Medical Imaging and Computer-Aided Diagnosis*, Ruidan Su, Yudong Zhang, Han Liu, and Alejandro F Frangi (Eds.). Springer Nature Singapore, Singapore, 293–303. https://doi.org/10.1007/978-981-16-6775-6_24

[31] Andre Mühlenbrock, Timur Cetin, Dirk Weyhe, and Gabriel Zachmann. 2022. Optimizing the arrangement of fixed light modules in new autonomous surgical lighting systems. In *Medical Imaging 2022: Image-Guided Procedures, Robotic Interventions, and Modeling*, Cristian A. Linte and Jeffrey H. Siewerdsen (Eds.), Vol. 12034. International Society for Optics and Photonics, SPIE, 491 – 499. https://doi.org/10.1117/12.2611058

[32] Angel Pachamanov and Dessislava Pachamanova. 2008. Optimization of the light distribution of luminaries for tunnel and street lighting. *Engineering Optimization* 40, 1 (2008), 47–65. https://doi.org/10.1080/03052150701591160

[33] Patkin. 2003. What surgeons want in operating rooms. *Minimally invasive therapy & allied technologies* 12, 6 (Nov 2003), 256–262. https://doi.org/10.1080/13645700310021133

[34] Martin Schlüter, Jose A. Egea, and Julio R. Banga. 2009. Extended ant colony optimization for non-convex mixed integer nonlinear programming. *Computers & Operations Research* 36, 7 (2009), 2217–2229. https://doi.org/10.1016/j.cor.2008.08.015

[35] Junfei Shen, Huihui Wang, Yisi Wu, An Li, Chi Chen, and Zhenrong Zheng. 2015. Surgical lighting with contrast enhancement based on spectral reflectance comparison and entropy analysis. *Journal of Biomedical Optics* 20, 10 (2015), 105012. https://doi.org/10.1117/1.JBO.20.10.105012

[36] Rainer Storn and Kenneth Price. 1997. Differential Evolution – A Simple and Efficient Heuristic for global Optimization over Continuous Spaces. *Journal of Global Optimization* 11, 4 (01 Dec 1997), 341–359. https://doi.org/10.1023/A:1008202821328

[37] Jörn Teuber, René Weller, Ron Kikinis, Karl-Jürgen Oldhafer, Michael J. Lipp, and Gabriel Zachmann. 2015. Autonomous Surgical Lamps. In *Jahrestagung der Deutschen Gesellschaft für Computer- und Roboterassistierte Chirurgie (CURAC)*. Bremen, Germany.

[38] Jörn Teuber, Rene Weller, Ron Kikinis, Karl-Jürgen Oldhafer, Michael J. Lipp, and Gabriel Zachmann. 2017. Optimized positioning of autonomous surgical lamps. In *Medical Imaging 2017: Image-Guided Procedures, Robotic Interventions, and Modeling*, Robert J. Webster III and Baowei Fei (Eds.), Vol. 10135. International Society for Optics and Photonics, SPIE, 1013513. https://doi.org/10.1117/12.2256029

[39] Cornelia Vandahl, Carsten Funke, Cornelia Moosmann, and Gemeinschaftstagung Licht ; 22 (Karlsruhe) : 2016.09.25-28. 2016. Einheitliche Bewertung von Lichtsituationen mit dem LiTG-Fragebogen - erste Erfahrungen. *Licht 2016: Karlsruhe, 25.-28. September* (2016), 27–34. https://doi.org/10.5445/KSP/1000057817

[40] H. Wang, R.H. Cuijpers, I.M.L.C. Vogels, M. Ronnier Luo, I. Heynderickx, and Z. Zheng. 2018. Optimising the illumination spectrum for tissue texture visibility. *Lighting Research & Technology* 50, 5 (2018), 757–771. https://doi.org/10.1177/1477153517690799

[41] Zizhen Wang and Yen Kheng Tan. 2013. Illumination control of LED systems based on neural network model and energy optimization algorithm. *Energy and Buildings* 62 (2013), 514–521. https://doi.org/10.1016/j.enbuild.2013.03.029

[42] Oliver Wasenmüller and Didier Stricker. 2017. Comparison of Kinect V1 and V2 Depth Images in Terms of Accuracy and Precision. In *Computer Vision – ACCV 2016 Workshops*, Chu-Song Chen, Jiwen Lu, and Kai-Kuang Ma (Eds.). Springer International Publishing, Cham, 34–45.

[43] Yao-Jung Wen and Alice M. Agogino. 2008. Wireless networked lighting systems for optimizing energy savings and user satisfaction. In *2008 IEEE Wireless Hive Networks Conference*. 1–7. https://doi.org/10.1109/WHNC.2008.4629493

[44] D.H. Wolpert and W.G. Macready. 1997. No free lunch theorems for optimization. *IEEE Transactions on Evolutionary Computation* 1, 1 (1997), 67–82. https://doi.org/10.1109/4235.585893

[45] Özgür Yeniay. 2005. Penalty Function Methods for Constrained Optimization with Genetic Algorithms. *Mathematical and Computational Applications* 10, 1 (2005), 45–56. https://doi.org/10.3390/mca10010045

[46] Nima Zargham, Tanja Döring, Anke V. Reinschluessel, Andre Mühlenbrock, Thomas Muender, Timur Cetin, Verena Nicole Uslar, Dirk Weyhe, and Rainer Malaka. 2024. Utilizing Gesture and Speech to Control Surgical Lighting Systems. (2024). Manuscript under review.

[47] Camilla Zetterberg, Marina Heiden, Per Lindberg, Per Nylén, and Hillevi Hemphälä. 2019. Reliability of a new risk assessment method for visual ergonomics. *International Journal of Industrial Ergonomics* 72 (2019), 71–79. https://doi.org/10.1016/j.ergon.2019.04.002